Ionospheric effects of magneto-acoustic-gravity waves: Dispersion relation

R. Michael Jones[a], Lev A. Ostrovsky[b,c], Alfred J. Bedard Jr.[a]

[a]*Cooperative Institute for Research in Environmental Sciences, University of Colorado, Boulder, Colorado 80309-0216, U.S.A.*
[b]*Applied Mathematics Department, University of Colorado, Boulder, Colorado 80309, U.S.A.*
[c]*Mathematics Department, University of North Carolina, Chapel Hill, U.S.A.*

Abstract

There is extensive evidence for ionospheric effects associated with earthquake-related atmospheric disturbances. Although the existence of earthquake precursors is controversial, one suggested method of detecting possible earthquake precursors and tsunamis is by observing possible ionospheric effects of atmospheric waves generated by such events. To study magneto-acoustic-gravity waves in the atmosphere, we have derived a general dispersion relation including the effects of the Earth's magnetic field. This dispersion relation can be used in a general atmospheric ray tracing program to calculate the propagation of magneto-acoustic-gravity waves from the ground to the ionosphere. The presence of the Earth's magnetic field in the ionosphere can radically change the dispersion properties of the wave. The general dispersion relation obtained here reduces to the known dispersion relations for magnetoacoustic waves and acoustic-gravity waves in the corresponding particular cases. The work described here is the first step in achieving a generalized ray tracing program permitting propagation studies of magneto-acoustic-gravity waves.

Keywords:
Magneto-acoustic-gravity waves, Magnetoacoustic waves, Acoustic-gravity waves, Ionosphere,

1. Introduction

Hines (1972) first suggested that atmospheric gravity waves generated by tsunamis might produce identifiable ionospheric signatures that could be used for tsunami warnings, and Peltier and Hines (1976) concluded that such a system might be practical after determining that the various difficulties were of only marginal consequence. Similarly, there have been a variety of earthquake-related infrasonic signals documented by past researchers. For example, epicentral-generated infrasound measured at long ranges (e.g. Young and Greene, 1982; Mikumo, 1968) and infrasound measured by the local passage of Rayleigh waves (e.g. Bedard, 1971; Cook, 1965; Liu et al., 2011). Also, secondary radiation of infrasound from Rayleigh waves interacting with complex terrain has been measured (e.g. Young and Greene, 1982; Le Pichon et al., 2002).

The predictions of Hines (1972), and Peltier and Hines (1976) have been verified by observations taken of ionospheric effects of tsunami-generated atmospheric gravity waves during several recent major earthquakes (for example Artru et al., 2005; Hickey, 2011; Mai and Kiang, 2009; Liu et al., 2011; Makela et al., 2011).

Arai et al. (2011) have measured a Lamb wave radiated by a tsunami epicentral ocean surface disturbance. They suggest that by monitoring acoustic-gravity waves associated with undersea seismic disturbances it may be possible to indicate the likelihood of tsunami generation.

Other precursors have also been suggested (Varotsos et al., 1993, 2003; Freund, 2003; Geller, 1996). Finally, not only can infrasound be generated directly by a tsunami, Le Pichon et al. (2005) documented infrasound generated by the process of a tsunami interacting with a shoreline.

If it were possible to detect earthquake precursors soon enough to give warnings, lives could be saved. One suggested method of detecting earthquake precursors is by observing possible effects on the ionosphere of atmospheric waves generated by earthquake precursors (Blaunstein and Hayakawa, 2009; Heki, 2011), but that method is controversial (Masci and Thomas, 2015).[1] Testing the feasibility of such a warning system requires being able to calculate the propagation of such atmospheric waves from the ground to the ionosphere. Ray tracing programs exist for calculating the propagation of acoustic-gravity waves (e.g. Bedard and Jones, 2013; Jones and Bedard, 2015; Jones et al., 1986a,b; Georges et al., 1990),[2] and estimates have been made for the propagation of acoustic/magneto-acoustic waves from the ground to the ionosphere (Ostrovsky, 2008). However, as far as we know, no ray tracing program is now available to calculate the propagation of magneto-acoustic-gravity waves or even just magnetoacoustic waves in the atmosphere. Here, we derive the appropriate dispersion relations that could be used in a ray tracing program to make such calculations.

Estimating the ionospheric effects of atmospheric waves began at least by the 1960s (Georges, 1967; Yeh and Liu, 1972).

[1]Because seismic (Rayleigh) waves propagate much faster than sound, they are presently monitored in some locations as a precursor in early warning systems. There are also warning systems based on monitoring the positions of strategically chosen points in an earthquake zone using GPS technology (e.g. Heki, 2011). Here, we consider the possibility of monitoring the ionosphere as an alternative, additional warning system.

[2]There are also programs for calculating the propagation of acoustic waves in the atmosphere that are not ray based.

Observation of atmospheric motions due to infrasound generation by earthquakes began as early as the 1960s. Due to the rapid decrease in gas density with altitude, the corresponding velocities and displacements can reach at least dozens of m/s and dozens of meters, respectively (Banister and Hereford, 1991; Pulinets, 2004; Krasnov et al., 2011; Rapoport et al., 2004; Heki, 2011, and the references therein). The role of magnetohydrodynamic effects in the evolution of infrasound entering the ionosphere from below had not been thoroughly studied until recently (Pokhotelov et al., 1995; Koshevaya et al., 2001; Ostrovsky, 2008). Ostrovsky (2008) analyzed the basic equations governing the propagation of sound from the ground to the ionosphere, and focused on understanding the main changes in the linear and nonlinear dynamics of an infrasonic wave propagating upward from the ground to ionospheric levels, where it transforms into the fast magnetic sound which is the same wave mode as the non-magnetic infrasound excited at lower altitudes. These calculations required some approximations, such as an exponential variation of density with height, a constant background magnetic field of the Earth, and making simple estimates for oblique propagation.

Here, we begin to extend the previous research by developing a general dispersion relation for magneto-acoustic-gravity waves, that could be used in an atmospheric ray tracing program to calculate the propagation of these waves from the ground up to the ionsophere. This will allow the calculations for arbitrary background models of temperature, density, pressure, winds, and the Earth's magnetic field, as well as extending the propagation to oblique propagation.

Hickey and Cole (1987) consider ionospheric mechanisms in more detail, including relative motion of ions and neutral molecules, as well as the role of viscosity and diffusion. Here we limit our approach to a simplified magnetohydrodynamic motion to apply to such sources as earthquake-generated magnetic sound.

Section 2 discusses how dispersion relations are used to construct WKB approximations following the method given by Weinberg (1962, Section IV). Section 3 gives the basic equations governing the propagation of magneto-acoustic-gravity waves. Section 4 linearizes the basic equations. Section 5 defines some of the notation.

Section 6 gives the dispersion relation for magneto-acoustic-gravity waves neglecting Coriolis force, vorticity, and rate-of-strain. This is later applied to examine wave properties for specific conditions.

Section 7 gives Hamilton's equations for the refraction and propagation of the rays that represent the waves determined by the system of coupled equations in section 4. It is pointed out that the dispersion relation can be used for the Hamiltonian in Hamilton's equations in a ray tracing program even if the dispersion relation is given as the determinant of a matrix because Jacobi's formula can be used for the derivative of a determinant.

Section 8 discusses growth and decay of the waves because it is necessary when deriving a dispersion relation to distinguish between actual growth or decay and apparent growth of the waves when propagating to a region of low atmospheric density. We are reminded that baroclinicity causes growth or decay of waves because buoyancy is not a conservative force in a baroclinic fluid. However, growth or decay of a wave caused by baroclinicity must result in energy exchange between the wave and the mean flow if dissipation terms are neglected.

Section 9 considers the special case of a current-free region (that is, a region in which there are no background currents). Equation (37) gives the magneto-acoustic-gravity-wave dispersion relation in a current-free region, which results in significant simplification. The resulting dispersion relation is used in further approximations to examine wave properties for specific conditions.

The barotropic approximation is often a good approximation for acoustic-gravity-wave propagation in the atmosphere. Section 10 applies the barotropic approximation to the dispersion relation, resulting in (38) for the more general case and (40) in a current-free region.

Section 11 investigates the properties of the barotropic approximation to the magneto-acoustic-gravity-wave dispersion relation. A key result is that the effect of the magnetic field increases with altitude as the Alfvén speed increases due to the decrease in atmospheric density with height.

Section 12 considers the special case of magnetoacoustic waves and shows exact agreement with the dispersion relation given in previous work (Ostrovsky, 2008). Section 13 considers Hamiltonian ray tracing of magnetoacoustic waves and shows that a quartic equation must be solved to give the magnitude of the wave vector to initialize the ray-path calculation when specifying the frequency and wave-normal direction.

Section 14 summarizes the main result, which is the derivation of the magneto-acoustic-gravity-wave dispersion relation, which is a generalization of the acoustic-gravity-wave dispersion relation to include a magnetic field, or the generalization of the magnetoacoustic-wave dispersion relation to include gravity.

Appendix A presents the linearized coupled equations in matrix form. The dissipation terms are neglected.

Appendix B gives the dispersion relation for magneto-acoustic-gravity waves in terms of the determinant of the matrix that represents the linearized coupled equations when the dissipation terms are neglected.

2. WKB approximations

Jones (1996) reviews the practical aspects of ray tracing, the WKB approximation, and the limits of geometrical optics to calculate wave propagation in the atmosphere. Although the WKB approximation was given its present name after 1926 (Wentzel, 1926; Kramers, 1926; Brillouin, 1926), the method was discovered earlier (Liouville, 1836, 1837a,b; Rayleigh (John William Strutt), 1912; Jeffreys, 1923).

There are several possibilities for calculating a dispersion relation for the waves associated with a system of differential equations. Sometimes it is possible to eliminate all of the dependent variables but one to get a single differential equation for one dependent variable. Alternatively, it is possible to use for the dispersion relation the determinant of a matrix based on the system of equations (e.g. Weinberg, 1962, Section IV), which is what we shall do here.

In either case, it is necessary to replace differential operators by frequencies or wavenumbers to get a dispersion relation. Although the choice of method leads to slightly different dispersion relations (Einaudi and Hines, 1970), resulting in slightly different ray paths, the resulting WKB approximations differ from one another by less than the error in the WKB approximation. There may be some controversy about whether a dispersion relation is unique (Einaudi and Hines, 1970; Godin, 2015; Weinberg, 1962; Jones, 2006).

The linearized momentum equation (9) in section 4 contains velocity shear terms that end up in the corresponding dispersion relation for the Eikonal method. Olbers (1981) reasons that in a WKB concept only the local fields are retained in the dispersion relation and gradients (such as shear terms) enter only the propagation and refraction equations. However, that restriction cannot apply when trying to construct approximate solutions to a differential equation that already contains gradient terms. He further reasons that keeping the shear terms in the dispersion relation would be inconsistent if those terms were smaller than some of the terms that are neglected in the WKB approximation. Although that reasoning is persuasive, a counter viewpoint is also persuasive. Namely, that to remove any of those shear terms from the differential equation or from the dispersion relation would lead to a WKB approximation for a different differential equation from the one intended. In that case, such a WKB approximation would not agree with the solution of the intended equation within the error in the WKB approximation.

Although the above consideration is sufficient to justify keeping all of the terms in the dispersion relation, there are some practical reasons for keeping the terms as well. It is sometimes necessary to keep some terms that may be small in some cases, but significant in other cases. Finally, even if some terms were always small, keeping all of the terms allows the dispersion relation to be written in a more compact form, and allows the dispersion relation to be more easily manipulated.

It is necessary to scale the dependent variables by factors of $\rho^{\pm 1/2}$ (Gossard and Hooke, 1975, p. 77) to avoid the appearance of extraneous growth or decay of the wave. This practice is supported by general physical reasoning based on $\rho(u^2 + v^2 + w^2)$ being proportional to kinetic energy density, reasoning that applies equally to barotropic and baroclinic flow. The components of the perturbation of the Earth's magnetic field are scaled by the background values in addition, for the same reason.

3. Basic equations

We use a pure magneto-hydrodynamic approximation, i.e. the plasma is locally neutral with infinite conductivity, and we do not consider separation between ions and neutral molecules. A more detailed analysis of the broad scope of problems related to the relative dynamics of ions and neutral components as well as dissipative processes in the ionosphere is beyond the framework of this paper, although it may be necessary to include them in the future for specific situations in the upper ionosphere.

The equations of magnetohydrodynamics result from combining the Navier-Stokes equations with Maxwell's equations and the Lorentz force equation, while taking the electric conductivity to be infinite and the magnetic permeability to be that of free space and assuming that the ions move with the neutral molecules[3] (Landau et al., 1984, Section 65).

Application of the equations of magnetohydrodynamics to the ionosphere, including the Earth's magnetic field gives the starting point for our development (Ostrovsky, 2008):

$$\frac{\partial \mathbf{U}}{\partial t} + (\mathbf{U}\cdot\nabla)\mathbf{U} + \frac{1}{\rho}\nabla\left(p + \frac{H^2}{8\pi}\right) - \frac{1}{4\pi\rho}(\mathbf{H}\cdot\nabla)\mathbf{H} - \mathbf{g} = \mathbf{L}_1 \qquad (1)$$

are the momentum equations, where $\mathbf{U}$ is the fluid velocity, ρ is the density, p is the pressure, $\mathbf{H}$ is the Earth's magnetic field, $\mathbf{g}$ is the vector gravitational field, and $\mathbf{L}_1$ is a dissipation term due to viscosity.

$$\frac{D\rho}{Dt} + \rho(\nabla\cdot\mathbf{U}) = 0 \qquad (2)$$

is the continuity equation, where the intrinsic derivative is defined by

$$\frac{D}{Dt} \equiv \frac{\partial}{\partial t} + \mathbf{U}\cdot\nabla\,. \qquad (3)$$

$$\frac{D\tilde{\rho}_{\mathrm{pot}}}{Dt} = 0 \qquad (4)$$

is the requirement that the fluid behaves adiabatically, where $\tilde{\rho}_{\mathrm{pot}}$ is the local potential density, defined by (Jones, 2001, 2005, 2006)

$$\nabla\tilde{\rho}_{\mathrm{pot}} = \nabla\rho - c_s^{-2}\nabla p\,, \qquad (5)$$

where c_s is the adiabatic sound speed, defined by (Yeh and Liu, 1972, eq. (8.1.16), p. 406), (Weinberg, 1972, eq. (15.8.17), p. 566)

$$c_s^2 = \left(\frac{\partial p}{\partial \rho}\right)\,, \qquad (6)$$

and the partial derivative is for constant entropy and constant chemical composition.

$$\frac{\partial \mathbf{H}}{\partial t} + (\mathbf{U}\cdot\nabla)\mathbf{H} - (\mathbf{H}\cdot\nabla)\mathbf{U} + \mathbf{H}(\nabla\cdot\mathbf{U}) = \mathbf{L}_2 \qquad (7)$$

and

$$(\nabla\cdot\mathbf{H}) = 0 \qquad (8)$$

give the behavior of the Earth's magnetic field, where $\mathbf{L}_2$ is a dissipation term due to electrical conductivity.

[3]The assumption that ions move with the neutral molecules will usually be true if the wavelength and wave period are much greater respectively than the mean free path and mean time between collisions. However, the development could be generalized by including ion-drag terms (Hickey and Cole, 1987).

4. Linearization

Our linearization of the equations mostly follows that of Landau et al. (1984, Section 69) and Ostrovsky (2008): We perturb the equations by letting $\mathbf{U} = \mathbf{U}_0 + \mathbf{u}$, $\mathbf{H} = \mathbf{H}_0 + \mathbf{h}$, $\rho = \rho_0 + \delta\rho$, $p = p_0 + \delta p$, and $\tilde{\rho}_{\rm pot} = \tilde{\rho}_{\rm pot\,0} + \delta\tilde{\rho}_{\rm pot}$.

A linearization of (1) is

$$\frac{D_0\mathbf{u}}{Dt} + (\mathbf{u}\cdot\nabla)\mathbf{U}_0 + \frac{1}{\rho_0}\nabla\left(\delta p + \frac{\mathbf{H}_0\cdot\mathbf{h}}{4\pi}\right) - \frac{1}{4\pi\rho_0}(\mathbf{H}_0\cdot\nabla)\mathbf{h} - \frac{1}{4\pi\rho_0}(\mathbf{h}\cdot\nabla)\mathbf{H}_0 - \tilde{\mathbf{g}}\frac{\delta\rho}{\rho_0} = \delta\mathbf{L}_1 \,, \quad (9)$$

where

$$\frac{D_0}{Dt} \equiv \frac{\partial}{\partial t} + \mathbf{U}_0\cdot\nabla \,, \quad (10)$$

and

$$\tilde{\mathbf{g}} \equiv \mathbf{g} - \frac{D_0\mathbf{U}_0}{Dt} = \frac{1}{\rho_0}\nabla\left(p_0 + \frac{H_0^2}{8\pi}\right) - \frac{1}{4\pi\rho_0}(\mathbf{H}_0\cdot\nabla)\mathbf{H}_0 = \frac{\nabla p_0}{\rho_0} + \frac{1}{4\pi\rho_0}\mathbf{H}_0\times(\nabla\times\mathbf{H}_0) \quad (11)$$

is the effective gravitational field, including (minus) the background acceleration of the fluid.

A linearization of (2) is

$$\frac{D_0\delta\rho}{Dt} + \rho_0(\nabla\cdot\mathbf{u}) - \frac{\delta\rho}{\rho_0}\frac{D_0\rho_0}{Dt} + (\mathbf{u}\cdot\nabla)\rho_0 = 0 \,. \quad (12)$$

A linearization of (4) is (Jones, 2001, 2005, 2006)

$$\frac{D_0\delta\tilde{\rho}_{\rm pot}}{Dt} + \mathbf{u}\cdot\nabla\tilde{\rho}_{\rm pot\,0} = 0 \,. \quad (13)$$

A linearization of (7) is

$$\frac{D_0\mathbf{h}}{Dt} + (\mathbf{u}\cdot\nabla)\mathbf{H}_0 - (\mathbf{H}_0\cdot\nabla)\mathbf{u} - (\mathbf{h}\cdot\nabla)\mathbf{U}_0 + \mathbf{H}_0(\nabla\cdot\mathbf{u}) + \mathbf{h}(\nabla\cdot\mathbf{U}_0) = \delta\mathbf{L}_2 \,. \quad (14)$$

In what follows, we neglect dissipative terms. This is justified in many cases for the upward propagating waves. For a brief discussion of the role of dissipation with the corresponding references, see Ostrovsky (2008). However, there may be situations where the dissipation terms are significant (e.g. Hickey and Cole, 1987). For relatively short-period infrasound, a radical increase in dissipation can be due to the nonlinearity which increases with height due to the decrease in air density and results in shock waves forming (Ostrovsky and Rubakha, 1972). However, we neglect nonlinear effects here.

Appendix A presents the linearized coupled equations in matrix form. Appendix B gives the dispersion relation for magneto-acoustic-gravity waves in terms of the determinant of the matrix that represents the linearized coupled equations following the method given by Weinberg (1962, Section IV). Equation (B.2) gives the magneto-acoustic-gravity-wave dispersion relation including Coriolis force, vorticity, and rate-of-strain. In the absence of the magnetic field, the dispersion relation reduces to that for acoustic-gravity waves (Jones, 2001, 2005, 2006).

From here on, we drop zero subscripts for compactness. All quantities without subscript from here on are background quantities.

5. Notation

We define several quantities that will be used later.

$$\mathbf{\Gamma} \equiv \mathbf{k}_A - \nabla p/(\rho c_s^2) \quad (15)$$

is the vector generalization (Jones, 2001) of Eckart's coefficient (Gossard and Hooke, 1975, p. 90) and

$$\tilde{\mathbf{\Gamma}} \equiv \mathbf{k}_A - \tilde{\mathbf{g}}/c_s^2 \,, \quad (16)$$

where $\mathbf{k}_A \equiv \nabla\rho/(2\rho)$.

The buoyancy frequency for a fluid that does not have an imposed magnetic field is the Brunt-Väisälä frequency, whose square is

$$N^2 = \nabla\tilde{\rho}_{\rm pot}\cdot\nabla p/\rho^2 = \mathbf{k}_B\cdot\nabla p/\rho \,, \quad (17)$$

where $\mathbf{k}_B \equiv \nabla\tilde{\rho}_{\rm pot}/\rho$. The buoyancy frequency $\tilde{N}$ for a fluid that has an imposed magnetic field is given by

$$\tilde{N}^2 = \nabla\tilde{\rho}_{\rm pot}\cdot\tilde{\mathbf{g}}/\rho = \mathbf{k}_B\cdot\tilde{\mathbf{g}} \,, \quad (18)$$

where $\tilde{\mathbf{g}}$ is given by (11), and includes some force terms from the magnetic field in addition to the gradient of pressure.

The acoustic cutoff frequency ω_a for a fluid that does not have an imposed magnetic field is given by

$$\omega_a^2 = c_s^2\Gamma^2 + N^2 = c_s^2\mathbf{k}_A^2 \,. \quad (19)$$

The corresponding frequency $\tilde{\omega}_a$ for a fluid that has an imposed magnetic field is given by

$$\tilde{\omega}_a^2 = c_s^2\mathbf{\Gamma}\cdot\tilde{\mathbf{\Gamma}} + \tilde{N}^2 \,. \quad (20)$$

6. Magneto-acoustic-gravity waves

For this development of magneto-acoustic-gravity waves, we neglect Coriolis force, vorticity, and rate-of-strain. That is, we take

$$\hat{\mathbf{M}} = \hat{\mathbf{M}}_1 + \hat{\mathbf{M}}_2 + \hat{\mathbf{M}}_3 + \mathbf{M}_6 \quad (21)$$

as defined in (A.3), (A.4), (A.5), and (A.8) in Appendix A, and

$$\mathbf{M} = \mathbf{M}_1 + \mathbf{M}_2 + \mathbf{M}_3 + \mathbf{M}_6 \quad (22)$$

as defined in (B.4), (B.5), (B.6), and (A.8) in the appendices. Multiplying the determinant of (22) by $c_s^2H_x^2H_y^2H_z^2/((4\pi\rho)^3\omega^2)$ and setting it to zero gives[4]

$$\begin{aligned}\omega^4 \Big[\omega^2 - c_s^2(\mathbf{k}+i\mathbf{\Gamma})\cdot(\mathbf{k}-i\tilde{\mathbf{\Gamma}}) - \mathbf{k_B}\cdot\tilde{\mathbf{g}} \\ -(\mathbf{H}\cdot\mathbf{k})^2/(4\pi\rho) - H^2k^2/(4\pi\rho)\Big] \\ +H^2k^2\omega^2(\mathbf{H}\cdot\mathbf{k})^2/(4\pi\rho)^2 \\ +c_s^2\omega^2\left[(\mathbf{k}+\mathbf{i\Gamma})\times\mathbf{k}_B\right]\cdot\Big[(\mathbf{k}-i\tilde{\mathbf{\Gamma}})\times\tilde{\mathbf{g}}\Big] \\ +c_s^2\omega^2\Big[+(\mathbf{k}+\mathbf{i\Gamma})\cdot(\mathbf{k}-i\tilde{\mathbf{\Gamma}})(\mathbf{k}\cdot\mathbf{H})^2 \\ +k^2(\mathbf{k}+\mathbf{i\Gamma})\cdot\mathbf{H}(\mathbf{k}-\mathbf{i}\tilde{\mathbf{\Gamma}})\cdot\mathbf{H}\Big]/(4\pi\rho)\end{aligned}$$

[4] as verified by an algebraic manipulation program (Mathematica)

$$
\begin{aligned}
&-c_s^2k^2(\mathbf{k}\cdot\mathbf{H})^2\left[(\mathbf{k}+\mathbf{i\Gamma})\cdot\mathbf{H}(\mathbf{k}-\mathbf{i\tilde{\Gamma}})\cdot\mathbf{H}\right]/(4\pi\rho)^2\\
&+\omega^2\left[+(\mathbf{k}_B\cdot\tilde{\mathbf{g}})(\mathbf{k}\cdot\mathbf{H})^2\right.\\
&\left.+k^2(\mathbf{H}\cdot\mathbf{k_B})(\mathbf{H}\cdot\tilde{\mathbf{g}})\right]/(4\pi\rho)\\
&-k^2(\mathbf{k}\cdot\mathbf{H})^2(\mathbf{H}\cdot\mathbf{k_B})(\mathbf{H}\cdot\tilde{\mathbf{g}})/(4\pi\rho)^2\\
&+\left[c_s^2\omega^2(\mathbf{k}\cdot\mathbf{H}\times\mathbf{\Gamma})(\mathbf{k}\cdot\mathbf{H}\times\tilde{\mathbf{\Gamma}})\right.\\
&+\omega^2(\mathbf{k}\cdot\mathbf{H}\times\mathbf{k_B})(\mathbf{k}\cdot\mathbf{H}\times\tilde{\mathbf{g}})\\
&-c_s^2H^2(\mathbf{k}\cdot\mathbf{\Gamma}\times\mathbf{k_B})(\mathbf{k}\cdot\tilde{\mathbf{\Gamma}}\times\tilde{\mathbf{g}})\\
&+c_s^2(\mathbf{k}\cdot\mathbf{H})(\mathbf{k}\cdot(\mathbf{k}+\mathbf{i\Gamma})\times\mathbf{k_B})(\mathbf{H}\cdot(\mathbf{k}-\mathbf{i\tilde{\Gamma}})\times\tilde{\mathbf{g}})\\
&+c_s^2(\mathbf{k}\cdot\mathbf{H})(\mathbf{H}\cdot(\mathbf{k}+\mathbf{i\Gamma})\times\mathbf{k_B})(\mathbf{k}\cdot(\mathbf{k}-\mathbf{i\tilde{\Gamma}})\times\tilde{\mathbf{g}})\\
&-c_s^2(\mathbf{k}\cdot\mathbf{H})^2((\mathbf{k}+\mathbf{i\Gamma})\times\mathbf{k_B})\cdot((\mathbf{k}-\mathbf{i\tilde{\Gamma}})\times\tilde{\mathbf{g}})\ ]/(4\pi\rho)\\
&=0\,. \qquad (23)
\end{aligned}
$$

We can partially factor (23) to give

$$
\begin{aligned}
&\left[\omega^2-\tfrac{(\mathbf{H\cdot k})^2}{4\pi\rho}\right]\Big\{\omega^2\left[\omega^2-c_s^2(\mathbf{k}+i\mathbf{\Gamma})\cdot(\mathbf{k}-i\tilde{\mathbf{\Gamma}})-\mathbf{k_B}\cdot\tilde{\mathbf{g}}\right.\\
&\left.-H^2k^2/(4\pi\rho)\right]\\
&+c_s^2\left[(\mathbf{k}+\mathbf{i\Gamma})\times\mathbf{k}_B\right]\cdot\left[(\mathbf{k}-\mathbf{i\tilde{\Gamma}})\times\tilde{\mathbf{g}}\right]\\
&+c_s^2\left[k^2(\mathbf{k}+\mathbf{i\Gamma})\cdot\mathbf{H}(\mathbf{k}-\mathbf{i\tilde{\Gamma}})\cdot\mathbf{H}\right]/(4\pi\rho)\\
&+\left[k^2(\mathbf{H}\cdot\mathbf{k_B})(\mathbf{H}\cdot\tilde{\mathbf{g}})\right]/(4\pi\rho)\Big\}\\
&+\left[c_s^2\omega^2(\mathbf{k}\cdot\mathbf{H}\times\mathbf{\Gamma})(\mathbf{k}\cdot\mathbf{H}\times\tilde{\mathbf{\Gamma}})\right.\\
&+\omega^2(\mathbf{k}\cdot\mathbf{H}\times\mathbf{k_B})(\mathbf{k}\cdot\mathbf{H}\times\tilde{\mathbf{g}})\\
&-c_s^2H^2(\mathbf{k}\cdot\mathbf{\Gamma}\times\mathbf{k_B})(\mathbf{k}\cdot\tilde{\mathbf{\Gamma}}\times\tilde{\mathbf{g}})\\
&+c_s^2(\mathbf{k}\cdot\mathbf{H})(\mathbf{k}\cdot(\mathbf{k}+\mathbf{i\Gamma})\times\mathbf{k_B})(\mathbf{H}\cdot(\mathbf{k}-\mathbf{i\tilde{\Gamma}})\times\tilde{\mathbf{g}})\\
&\left.+c_s^2(\mathbf{k}\cdot\mathbf{H})(\mathbf{H}\cdot(\mathbf{k}+\mathbf{i\Gamma})\times\mathbf{k_B})(\mathbf{k}\cdot(\mathbf{k}-\mathbf{i\tilde{\Gamma}})\times\tilde{\mathbf{g}})\right]/(4\pi\rho)\\
&=0\,. \qquad (24)
\end{aligned}
$$

We use

$$
\mathbf{\Gamma}\times\mathbf{k}_B=\mathbf{k}_B\times\nabla p/(2\rho c_s^2)=\mathbf{B}/(2c_s^2) \qquad (25)
$$

and

$$
\tilde{\mathbf{\Gamma}}\times\tilde{\mathbf{g}}=\mathbf{k}_A\times\tilde{\mathbf{g}}=\tilde{\mathbf{B}}_2/2 \qquad (26)
$$

in (24) to give

$$
\begin{aligned}
&\left[\omega^2-\tfrac{(\mathbf{H\cdot k})^2}{4\pi\rho}\right]\Big\{\omega^2\left[\omega^2-c_s^2k^2-\tilde{\omega}_a^2-i\mathbf{k}\cdot(\tilde{\mathbf{g}}-\nabla p/\rho)\right.\\
&\left.-H^2k^2/(4\pi\rho)\right]\\
&+c_s^2\left[k^2\tilde{N}^2-\mathbf{k}\cdot\mathbf{k}_B\mathbf{k}\cdot\tilde{\mathbf{g}}+\mathbf{B}\cdot\tilde{\mathbf{B}}_2/(4c_s^2)\right.\\
&\left.+i\mathbf{k}\cdot\left(\tilde{\mathbf{B}}_2\times\mathbf{k}_B-\mathbf{B}\times\tilde{\mathbf{g}}/c_s^2\right)/2\right]\\
&+c_s^2\left[k^2(\mathbf{k}+\mathbf{i\Gamma})\cdot\mathbf{H}(\mathbf{k}-\mathbf{i\tilde{\Gamma}})\cdot\mathbf{H}\right]/(4\pi\rho)\\
&+\left[k^2(\mathbf{H}\cdot\mathbf{k_B})(\mathbf{H}\cdot\tilde{\mathbf{g}})\right]/(4\pi\rho)\Big\}\\
&+\left[c_s^2\omega^2(\mathbf{k}\cdot\mathbf{H}\times\mathbf{\Gamma})(\mathbf{k}\cdot\mathbf{H}\times\tilde{\mathbf{\Gamma}})\right.\\
&+\omega^2(\mathbf{k}\cdot\mathbf{H}\times\mathbf{k_B})(\mathbf{k}\cdot\mathbf{H}\times\tilde{\mathbf{g}})\\
&-c_s^2H^2(\mathbf{k}\cdot\mathbf{B})(\mathbf{k}\cdot\tilde{\mathbf{B}}_2)/(4c_s^2)\\
&+ic_s^2(\mathbf{k}\cdot\mathbf{H})(\mathbf{k}\cdot\mathbf{B})\left(\mathbf{H}\cdot(\mathbf{k}\times\tilde{\mathbf{g}}-i\tilde{\mathbf{B}}_2/2)\right)/(2c_s^2)\\
&\left.-ic_s^2(\mathbf{k}\cdot\mathbf{H})\left(\mathbf{H}\cdot\left(\mathbf{k}\times\mathbf{k}_B+i\mathbf{B}/(2c_s^2)\right)\right)(\mathbf{k}\cdot\tilde{\mathbf{B}}_2)/2\right]/(4\pi\rho)\\
&=0 \qquad (27)
\end{aligned}
$$

for the dispersion relation, where the baroclinic vectors $\mathbf{B}$ and $\tilde{\mathbf{B}}_2$ are defined in (34) and (36) in section 8.

Setting the magnetic field to zero in (27) agrees with the usual dispersion relation for acoustic-gravity waves in a baroclinic fluid (Jones, 2005, equation 11) and (Jones, 2006, equation 5) when the effects of vorticity, rotation of the Earth, and rate-of-strain are neglected.

We shall consider in section 11 how the details of (27) can give us insight into the propagation of magneto-acoustic-gravity waves.

7. Hamiltonian ray tracing

In Hamiltonian ray tracing, the ray paths are determined by Hamilton's equations.

$$
\frac{dx_i}{d\tau}=\frac{\partial H(t,x_i,\sigma,k_i)}{\partial k_i}\,, \qquad (28)
$$

$$
\frac{dk_i}{d\tau}=-\frac{\partial H(t,x_i,\sigma,k_i)}{\partial x_i}\,, \qquad (29)
$$

$$
\frac{dt}{d\tau}=-\frac{\partial H(t,x_i,\sigma,k_i)}{\partial \sigma}\,, \qquad (30)
$$

and

$$
\frac{d\sigma}{d\tau}=\frac{\partial H(t,x_i,\sigma,k_i)}{\partial t}\,, \qquad (31)
$$

where i varies from 1 to 3, τ is an independent variable whose significance depends on the choice of Hamiltonian, $H(t,x_i,\sigma,k_i)$, and these equations are integrated numerically along the ray path. Equation (28) gives the progression of the ray, (29) gives the refraction of the wave normal, (30) gives the travel time of the time-maximum of a wave packet (Hines, 1951a,b), and (31) gives the frequency shift of the wave if the medium is changing with time.

(Misner et al., 1973, p. 488) refer to the Hamiltonian in (28) through (31) as a super-Hamiltonian. The difference is that a normal Hamiltonian is three-dimensional, represents energy, and varies along the path, whereas a super-Hamiltonian is four-dimensional and is a constant (equal to zero) along the path.

Because it is necessary to choose for the Hamiltonian something that should be constant along the ray path, it is usual to choose some form of the dispersion relation for a Hamiltonian. Here, is is useful to take

$$
H(t,x_i,\sigma,k_i)=c_s^2H_x^2H_y^2H_z^2\,|\mathbf{M}|\,/((4\pi\rho)^3\omega^2)=0 \qquad (32)
$$

for the Hamiltonian, where the matrix $\mathbf{M}$ is defined in (22). There will be no confusion between the Hamiltonian $H(t,x_i,\sigma,k_i)$ and the Earth's magnetic field $\mathbf{H}$.

Unless attenuation of a wave is a significant cause of refraction (as it is for low-frequency radio waves in the ionospheric D region (Jones, 1970)), the imaginary part of the Hamiltonian can be neglected for calculating ray paths, and used only for calculating attenuation of the wave (or amplification of the wave when there is transfer of energy from the mean flow to the wave).

Although the determinant defining the Hamiltonian in (32) could be expanded out to give a more explicit form for the Hamiltonian, it would be tedious for an 8×8 determinant, and is not necessary because the derivatives of a determinant necessary to calculate Hamilton's equations can be expressed explicitly in terms of the trace of derivatives of the elements of the corresponding matrix times the inverse of the matrix using Jacobi's formula (e.g. Magnus and Neudecker, 1988, Part 3, Section 8.3, p. 149).

An appropriate computer program to calculate ray paths using the dispersion relation in (32) is the general three-dimensional ray tracing program for calculating acoustic-gravity waves in the atmosphere (described in Bedard and Jones, 2013; Jones and Bedard, 2015) based on an earlier program for calculating the propagation of acoustic waves (Jones et al., 1986a,b; Georges et al., 1990). In addition to adding to that ray tracing program the dispersion relation defined by the Hamiltonian in (32), it would be necessary to add a model for the Earth's magnetic field.

Although dissipation is neglected here, there can be growth or decay of the wave because of energy exchange between the wave and the mean flow. This is shown by the complex dispersion relation, which leads to a complex phase refractive index, a complex group refractive index, and a complex group velocity. Although the significance of a complex phase refractive index is well known, the significance of a complex group refractive index and a complex group velocity are less well known. The group refractive index n' can be defined as

$$n' = \frac{c_{\mathrm{ref}}}{\partial\omega/\partial\mathbf{k}} , \tag{33}$$

where c_{ref} is an arbitrary reference speed, and $\partial\omega/\partial\mathbf{k}$ is group velocity.

Hines (1951a,b) showed that the speed of the time-maximum of a pulse was equal to the reference speed divided by the real part of the group refractive index. That is, the travel time of the time-maximum of a pulse is proportional to the integral along the ray path of the real part of the group refractive index.

The significance of the imaginary part of the complex group refractive index is less well known. The group refractive index will be complex if the wave growth or decay depends on frequency. A pulse propagating through a medium that has a complex group refractive index will have its frequency shifted by an amount that is proportional to the imaginary part of the group refractive index (Jones, 1981)

8. Energy exchange between the waves and the mean flow

Usually, imaginary terms in a dispersion relation represent growth or decay of the wave. Sometimes those imaginary terms are extraneous, caused by not correctly scaling some of the variables. For example, not scaling some variables by the square root of the density can cause extraneous growth or decay of the wave.

Without extraneous growth or decay, imaginary terms in the dispersion relation are due to either dissipation, or energy exchange between the wave and the background flow. Because dissipation has been neglected here, growth or attenuation of the wave must be associated with energy exchange between the wave and the background flow. There is then the question of whether we are violating the non-acceleration theorem, which we now address.

The non-acceleration theorem states that steady, non-dissipated, long, quasi-static, stationary waves have no effect on the mean (zonally averaged) flow (Eliassen and Palm, 1960; Andrews, 2009). Or, in a related statement (Charney and Drazin, 1961) "However, when the wave disturbance is a small stationary perturbation on a zonal flow that varies vertically but not horizontally, the second-order effect of the eddies on the zonal flow is zero." It seems clear from the above statements, that although the non-acceleration theorem is important and has wide applicability, it does not prohibit coupling between the wave and the mean flow in all cases. In particular, Jones (2001, Sections IV and V) presents a parcel explanation to show that buoyancy is a non-conservative force in a baroclinic fluid, which implies energy exchange between a wave and the mean flow. In addition, Jones (2001, Sections IV and V) uses the vorticity equation to show that baroclinicity contributes to a time variation of vorticity, and estimates the time-rate-of-change of the action to show why we should expect energy exchange between the wave and the background flow in a baroclinic fluid. The generalized Eliassen-Palm and Charney-Drazin theorems (Andrews and McIntyre, 1976, 1978) also do not prohibit coupling between the wave and the mean flow in all cases.

If the matrix $\hat{\mathbf{M}}$ in (A.2) is Hermitian (that is, if the real part of the matrix is symmetric and the imaginary part is antisymmetric), then the waves will propagate without growth or attenuation. Because $\hat{\mathbf{M}}_1$, $\hat{\mathbf{M}}_2$, and $\hat{\mathbf{M}}_3$ are symmetric, $\hat{\mathbf{M}}$ will be Hermitian if all of the other matrices (which are all imaginary) are antisymmetric.

For a fluid that does not have an imposed magnetic field, the fluid is barotropic if ∇p is in the same direction as $\nabla\rho$. On the other hand, the fluid is baroclinic if the gradients of pressure and density are inclined to each other. Specifically, the baroclinic vector is defined as

$$\mathbf{B} \equiv \nabla\rho\times\nabla p/\rho^2 = \nabla\tilde{\rho}_{\mathrm{pot}}\times\nabla p/\rho^2 = 2\mathbf{k}_A\times\nabla p/\rho = \mathbf{k}_B\times\nabla p/\rho \; . \tag{34}$$

For a fluid that has an imposed magnetic field, there is more than one way that the fluid can be baroclinic because the direction of the magnetic field and its gradient give additional independent vectors that might or might not be in the same direction as the gradients of pressure or density. There are, in that general case, three independent vectors, and three independent pairs of those vectors, that leads to three independent baroclinic vectors. Specifically, in addition to the baroclinic vector defined in (34), we also have another baroclinic vector $\tilde{\mathbf{B}}_1$ defined by

$$\tilde{\mathbf{B}}_1 \equiv \nabla\tilde{\rho}_{\mathrm{pot}} \times \tilde{\mathbf{g}}/\rho = \mathbf{k}_B \times \tilde{\mathbf{g}} \; , \tag{35}$$

and another baroclinic vector $\tilde{\mathbf{B}}_2$ defined by

$$\tilde{\mathbf{B}}_2 \equiv \nabla\rho \times \tilde{\mathbf{g}}/\rho = 2\mathbf{k}_A \times \tilde{\mathbf{g}} \; , \tag{36}$$

both of which differ from the baroclinic vector defined in (34) when the curl of the magnetic field is non-zero, as can be seen from (11).

The matrix $\mathbf{M}_6$ in (A.8) would be antisymmetric if the flow were barotropic ($\mathbf{B}$, $\tilde{\mathbf{B}}_1$, and $\tilde{\mathbf{B}}_2$ all equal to zero) and if $\tilde{\mathbf{\Gamma}} = \mathbf{\Gamma}$. The matrix $\mathbf{M}_6$ in (A.8) will have a symmetric component if the wave is baroclinic (any of $\mathbf{B}$, $\tilde{\mathbf{B}}_1$, or $\tilde{\mathbf{B}}_2$ being non-zero) or if $\tilde{\mathbf{\Gamma}} \neq \mathbf{\Gamma}$.

Because $\mathbf{M}_4$ and $\mathbf{M}_8$ in (A.6) and (A.11) are antisymmetric, they will not contribute to energy exchange between the wave and the mean flow. Because $\mathbf{M}_5$ and $\mathbf{M}_{12}$ in (A.7) and (A.15) are symmetric, they could contribute to energy exchange between the wave and the mean flow, but that would require magnetic monopoles and the creation of matter in the atmosphere.

That the symmetric rate of strain tensor (A.10) in the matrix $\mathbf{M}_7$ in (A.9) can contribute to energy exchange between the wave and the background flow follows from the relationship among Reynolds stress, eddy viscosity, and the symmetric rate of strain tensor (Monin and Yaglom, 1987, section 6.3, p. 389). The rest of the matrix $\mathbf{M}_7$ in (A.9) is antisymmetric, so it will not contribute to energy exchange between the wave and the mean flow.

Because $\mathbf{M}_9$ and $\mathbf{M}_{11}$ in (A.12) and (A.14) have symmetric components, they can contribute to energy exchange between the wave and the mean flow. The matrix $\mathbf{M}_{10}$ in (A.13) can contribute to energy exchange between the wave and the mean flow unless the curl of the Earth's magnetic field is zero. However, Maxwell's equations would then require there to be electric currents or a time-varying electric field, which would explain why such a term might lead to energy exchange between the wave and the background.

9. Current-free background

The contribution of the background magnetic field to the effective background gravitational field $\tilde{\mathbf{g}}$ in (11) is proportional to the curl of the magnetic field. However, one of Maxwell's equations tells us that the curl of the magnetic field is zero in any region that is free of electric currents if the electric field is not changing with time. For the case of a current-free background, the contribution of the magnetic field to the effective gravitational field $\tilde{\mathbf{g}}$ in (11) is also zero.

In that case, we get $\tilde{\mathbf{g}} = \nabla p/\rho$, which gives $\tilde{\mathbf{\Gamma}} = \mathbf{\Gamma}$, $\tilde{N} = N$, $\tilde{\omega}_a = \omega_a$, and $\tilde{\mathbf{B}}_1 = \tilde{\mathbf{B}}_2 = \mathbf{B}$, which results in a great deal of simplification in the dispersion relation in (27). This gives

$$
\begin{aligned}
&\left[\omega^2 - \tfrac{(\mathbf{H}\cdot\mathbf{k})^2}{4\pi\rho}\right]\Big\{\omega^2\left[\omega^2 - c_s^2k^2 - \omega_a^2 - H^2k^2/(4\pi\rho)\right] \\
&\quad +c_s^2\left[k^2N^2 - \mathbf{k}\cdot\mathbf{k}_B\mathbf{k}\cdot\tilde{\mathbf{g}} + \mathbf{B}\cdot\mathbf{B}/(4c_s^2)\right. \\
&\quad \left. +i\mathbf{k}\cdot\left(\mathbf{B}\times\mathbf{k}_B - \mathbf{B}\times\tilde{\mathbf{g}}/c_s^2\right)/2\right] \\
&\quad +c_s^2\left[k^2(\mathbf{k}+i\mathbf{\Gamma})\cdot\mathbf{H}(\mathbf{k}-i\mathbf{\Gamma})\cdot\mathbf{H}\right]/(4\pi\rho) \\
&\quad +\left[k^2(\mathbf{H}\cdot\mathbf{k_B})(\mathbf{H}\cdot\tilde{\mathbf{g}})\right]/(4\pi\rho)\Big\} \\
&+\left[c_s^2\omega^2(\mathbf{k}\cdot\mathbf{H}\times\mathbf{\Gamma})^2 + \omega^2(\mathbf{k}\cdot\mathbf{H}\times\mathbf{k_B})(\mathbf{k}\cdot\mathbf{H}\times\tilde{\mathbf{g}})\right. \\
&\quad -c_s^2H^2(\mathbf{k}\cdot\mathbf{B})^2/(4c_s^2) \\
&\quad +ic_s^2(\mathbf{k}\cdot\mathbf{H})(\mathbf{k}\cdot\mathbf{B})\left(\mathbf{H}\cdot(\mathbf{k}\times\tilde{\mathbf{g}} - i\mathbf{B}/2)\right)/(2c_s^2) \\
&\quad \left. -ic_s^2(\mathbf{k}\cdot\mathbf{H})\left(\mathbf{H}\cdot\left(\mathbf{k}\times\mathbf{k}_B + i\mathbf{B}/(2c_s^2)\right)\right)(\mathbf{k}\cdot\mathbf{B})/2\right]/(4\pi\rho) \\
&= 0 \qquad (37)
\end{aligned}
$$

for the dispersion relation.

10. Barotropic approximation

The barotropic approximation is usually valid for acoustic-gravity waves whenever Coriolis effects can be neglected. It is likely that the barotropic approximation is also valid for magneto-acoustic-gravity waves whenever Coriolis effects can be neglected. We make the barotropic approximation by neglecting the baroclinic vectors $\mathbf{B}$ and $\tilde{\mathbf{B}}_2$ in (27). This gives

$$
\begin{aligned}
&\left[\omega^2 - \tfrac{(\mathbf{H}\cdot\mathbf{k})^2}{4\pi\rho}\right]\Big\{\omega^2\left[\omega^2 - c_s^2k^2 - \tilde{\omega}_a^2 - i\mathbf{k}\cdot(\tilde{\mathbf{g}} - \nabla p/\rho)\right. \\
&\quad \left. -H^2k^2/(4\pi\rho)\right] + c_s^2\left[k^2\tilde{N}^2 - \mathbf{k}\cdot\mathbf{k}_B\mathbf{k}\cdot\tilde{\mathbf{g}}\right] \\
&\quad +c_s^2\left[k^2(\mathbf{k}+i\mathbf{\Gamma})\cdot\mathbf{H}(\mathbf{k}-i\tilde{\mathbf{\Gamma}})\cdot\mathbf{H}\right]/(4\pi\rho) \\
&\quad +\left[k^2(\mathbf{H}\cdot\mathbf{k_B})(\mathbf{H}\cdot\tilde{\mathbf{g}})\right]/(4\pi\rho)\Big\} \\
&\quad +\left[c_s^2\omega^2(\mathbf{k}\cdot\mathbf{H}\times\mathbf{\Gamma})(\mathbf{k}\cdot\mathbf{H}\times\tilde{\mathbf{\Gamma}})\right. \\
&\quad \left. +\omega^2(\mathbf{k}\cdot\mathbf{H}\times\mathbf{k_B})(\mathbf{k}\cdot\mathbf{H}\times\tilde{\mathbf{g}})\right]/(4\pi\rho) \\
&= 0\,. \qquad (38)
\end{aligned}
$$

The barotropic approximation for the dispersion relation for a current-free background, from (37), is

$$
\begin{aligned}
&\left[\omega^2 - \tfrac{(\mathbf{H}\cdot\mathbf{k})^2}{4\pi\rho}\right]\Big\{\omega^2\left[\omega^2 - c_s^2k^2 - \omega_a^2 - H^2k^2/(4\pi\rho)\right] \\
&\quad +c_s^2\left[k^2N^2 - \mathbf{k}\cdot\mathbf{k}_B\mathbf{k}\cdot\tilde{\mathbf{g}}\right] \\
&\quad +c_s^2\left[k^2(\mathbf{k}+i\mathbf{\Gamma})\cdot\mathbf{H}(\mathbf{k}-i\mathbf{\Gamma})\cdot\mathbf{H}\right]/(4\pi\rho) \\
&\quad +\left[k^2(\mathbf{H}\cdot\mathbf{k_B})(\mathbf{H}\cdot\tilde{\mathbf{g}})\right]/(4\pi\rho)\Big\} \\
&\quad +\left[c_s^2\omega^2(\mathbf{k}\cdot\mathbf{H}\times\mathbf{\Gamma})^2\right. \\
&\quad \left. +\omega^2(\mathbf{k}\cdot\mathbf{H}\times\mathbf{k_B})(\mathbf{k}\cdot\mathbf{H}\times\tilde{\mathbf{g}})\right]/(4\pi\rho) \\
&= 0\,. \qquad (39)
\end{aligned}
$$

Rearranging terms and making appropriate substitutions in (39) gives

$$
\begin{aligned}
&\left(\omega^2 - c_A^2k_H^2\right)\Big[(\omega^2-\omega_a^2)\left(\omega^2 - c_A^2k^2\right) \\
&\quad +c_s^2(N^2(k_x^2+k_y^2) - \omega^2k^2) \\
&\quad +c_A^2k^2(-\omega_a^2(H_x^2+H_y^2)/H^2 + c_s^2k_H^2)\Big] \\
&\quad +k_\perp^2c_A^2\omega^2\omega_a^2(H_x^2+H_y^2)/H^2 = 0\,, \qquad (40)
\end{aligned}
$$

where k_H is the component of $\mathbf{k}$ in the direction of $\mathbf{H}$, H_x and H_y are the components of $\mathbf{H}$ perpendicular to $\mathbf{k}_B$ and $\tilde{\mathbf{g}}$, k_x and k_y are the components of $\mathbf{k}$ perpendicular to $\mathbf{k}_B$ and $\tilde{\mathbf{g}}$, $k_\perp$ is the component of $\mathbf{k}$ perpendicular to both $\mathbf{k}_B$ (and $\tilde{\mathbf{g}}$) and $\mathbf{H}$, and

$$
\mathbf{c}_A = \frac{\mathbf{H}}{\sqrt{4\pi\rho}} \qquad (41)
$$

is the Alfvén velocity.

Notice that the dispersion relation for the Alfvén wave factors out only if the wave vector $\mathbf{k}$ is in the plane of $\mathbf{k}_B$ (and $\tilde{\mathbf{g}}$) and $\mathbf{H}$ (making the last term zero). Setting c_A to zero in (40) gives the usual barotropic acoustic-gravity-wave dispersion relation (e.g. Eckart, 1960; Gossard and Hooke, 1975; Jones, 2001, 2005, 2006). Setting both N and ω_a to zero in (40) gives the dispersion relation for magnetoacoustic waves and Alfvén waves (61).

Ordinary sound transforms to magnetic sound smoothly with no discontinuities. Gravity waves do not couple with acoustic waves because there is a frequency gap between the Brunt-Väisälä frequency and the acoustic-cutoff frequency. However, there is not always a frequency gap between magnetogravity waves and magnetoacoustic waves under some circumstances.

11. Properties of the magneto-acoustic-gravity wave dispersion relation

Now we consider more specific dispersion properties of magneto-acoustic-gravity waves in several quantitative examples. Here we neglect Coriolis force and concentrate on three factors which are characteristic of the relatively short-period waves excited by the ground and water motions affecting the ionosphere, namely the compressibility, magnetic field, and gravity.

To determine the properties of the magneto-acoustic-gravity wave dispersion relation, it is useful to choose a coordinate system in which the magnetic field is in the $x-z$ frame. Then, we can write (40) as

$$\begin{aligned}
&\left[\omega^2 - c_A^2 k_H^2\right]\Big\{(\omega^2-\omega_a^2)\omega^2 \\
&+k_x^2\left[N^2c_s^2 - \omega^2(c_s^2+c_A^2) + c_A^2\omega_a^2\cos^2\phi + c_A^2c_s^2k_H^2\right] \\
&+k_y^2\left[N^2c_s^2 - \omega^2(c_s^2+c_A^2) + c_A^2\omega_a^2\cos^2\phi + c_A^2c_s^2k_H^2\right] \\
&+k_z^2\left[-\omega^2(c_s^2+c_A^2) + c_A^2\omega_a^2\cos^2\phi + c_A^2c_s^2k_H^2)\right]\Big\} \\
&+k_y^2c_A^2\omega^2\omega_a^2\sin^2\phi = 0\,, \qquad (42)
\end{aligned}$$

where ϕ is the angle between the magnetic field and the z axis, and

$$k_H^2 = k_x^2\sin^2\phi + 2k_xk_z\sin\phi\cos\phi + k_z^2\cos^2\phi\,. \qquad (43)$$

A symmetric form, equivalent to (42), that we shall use later to explain some of the figures is

$$\begin{aligned}
&\left(\frac{k^2-k_H^2}{\omega^2} + \frac{k_A^2\sin^2\phi}{\omega^2} - \frac{(k_x^2+k_y^2)N^2}{\omega^4}\right)\left(\frac{1}{c_s^2} + \frac{1}{c_A^2} - \frac{k_H^2}{\omega^2} - \frac{k_A^2\cos^2\phi}{\omega^2}\right) \\
&-\left(\frac{1}{c_s^2} - \frac{k_H^2}{\omega^2} - \frac{k_A^2\cos^2\phi}{\omega^2}\right)\left(\frac{1}{c_A^2} - \frac{k_H^2}{\omega^2} + \frac{k_A^2\sin^2\phi}{\omega^2} - \frac{(k_x^2+k_y^2)N^2}{\omega^4}\right) \\
&+\frac{k_y^2}{\omega^2}\frac{k_A^2\sin^2\phi}{\omega^2-c_A^2k_H^2} = 0\,. \qquad (44)
\end{aligned}$$

11.1. In the $k_x - k_z$ plane

For propagation in the $k_x - k_z$ plane, the last term in (42) is zero. In that case, the rest of (42) factors. The second factor is

$$\begin{aligned}
&[\omega^2-\omega_a^2]\omega^2 \\
&+\left[N^2c_s^2 - \omega^2(c_s^2+c_A^2) + c_A^2\omega_a^2\cos^2\phi + c_A^2c_s^2k_H^2\right]k_x^2 \\
&+\left[-\omega^2(c_s^2+c_A^2) + c_A^2\omega_a^2\cos^2\phi + c_A^2c_s^2k_H^2\right]k_z^2 \\
&= 0\,. \qquad (45)
\end{aligned}$$

Equation (45) can tell us under what conditions waves are propagating or evanescent. If the coefficients (the factors in brackets) of all three terms in (45) are the same sign, then the waves will be evanescent because that would require at least one of ω^2, k_x^2, or k_z^2 to be negative. For very large frequency, the first coefficient will be positive and the other two coefficients will be negative, to give a propagating acoustic wave or magnetoacoustic wave depending on other conditions. As the frequency is lowered, one or more of the coefficients will eventually change sign. If the first coefficient changes sign first (which it will when c_A is small enough), then the wave will become evanescent, and the wave will remain evanescent until the frequency is lowered enough that one of the other coefficients changes sign, which usually occurs at the Brunt-Väisälä frequency, N, when c_A is small enough. When c_A is larger, there might not be any frequencies for which all three coefficients are the same sign, and therefore no frequencies for which the wave is evanescent. However, even then, gravity would still have a significant effect on the propagation at some frequencies through the N and ω_a terms.

We present here a set of figures to illustrate the effects of the magnetic field on acoustic-gravity-wave propagation. Since the Alfvén speed c_A varies approximately exponentially with height (because it is proportional to the reciprocal of the square root of density), its height variation will dominate the height variation of the dispersion relation. To illustrate that dependence, we have chosen values of c_A that represent its value at various heights in the atmosphere. The first two figures show the dispersion relation for gravity waves at heights of about 95 km and 115 km to show how the effect of the magnetic field on gravity waves increases with height. The next four figures show the dispersion relation for normal sound and magnetic sound just below and just above the height (about 155 km) where normal sound couples to magnetic sound because c_A is equal to c_s, the sound speed there.

One way to look at the dispersion relation is to consider frequency to be a function of the components of the wavenumber. For that, we write (45) as

$$\begin{aligned}
&\omega^4 - \omega^2\left[\omega_a^2 + (c_s^2+c_A^2)(k_x^2+k_z^2)\right] \\
&+k_x^2\left[N^2c_s^2 + c_A^2\omega_a^2\cos^2\phi + c_A^2c_s^2k_H^2\right] \\
&+k_z^2\left[c_A^2\omega_a^2\cos^2\phi + c_A^2c_s^2k_H^2\right] \\
&= 0\,. \qquad (46)
\end{aligned}$$

Equation (46) can be solved as a quadratic equation for ω^2 as a function of k_x and k_z. The results are shown as three-dimensional surface plots in figures 1 through 4 for various values of the parameters. In addition, the intersections of those surfaces with a horizontal plane for a specific frequency is shown.

Figures 1 and 2 show the intersection of the dispersion-relation surface with a plane that corresponds to an intrinsic frequency below the acoustic cutoff frequency, while figures 3 and 4 show a similar intersection for an intrinsic frequency above the acoustic cutoff frequency. Note that in the low-frequency case only one propagating wave mode exists, whereas at higher frequencies and larger c_A there are two propagating modes. Figure 5 shows both these modes (intersections) in the form of the dispersion curves relating k_x and k_z for a frequency of 0.01 Hz. For all of these figures, the sound speed, $c_s = 0.3$ km s^{-1}, the Brunt-Väisälä frequency, $N = 0.01$ s^{-1}, $\cos^2\phi = 0.5$, $k_A = 0.035$ km^{-1}, and the acoustic cutoff frequency, $\omega_a = 0.0105$ rad s^{-1}.

The cases in figures 1 and 2 can be interpreted as a mixture of magnetogravity waves and magnetoacoustic waves. Near the origin, we see the dispersion relation for magnetogravity waves, which resembles that for non-magnetic gravity waves. However, the magneto-gravity waves switch to magneto-acoustic waves away from the origin.

The case in figure 2 is the same as that in figure 1 except that the Alfvén speed is larger in figure 2, leading to a larger effect from the magnetic field. Generally, the effect of the magnetic field increases with height in the atmosphere as the Alfvén speed increases because it is inversely proportional to the square root of density.

Figure 3 shows the dispersion relation for the slow magnetoacoustic wave. The direction of the magnetic field is approximately perpendicular to the two nearly parallel lines. It would be exactly perpendicular if there were no effect of the gravitational field.

Figure 4 shows the dispersion relation for the fast magnetoacoustic wave. The radius of the small "circle" is approximately $\sqrt{\omega^2/c_s^2 - k_A^2\cos^2\phi}$ ($\approx \omega/c_s$ for the values in figure 4) parallel to the magnetic field, but the radius is approximately $\omega/\sqrt{c_s^2 + c_A^2}$ normal to the magnetic field (when the effect of gravity can be neglected). The fast magnetoacoustic wave becomes an ordinary acoustic wave as $c_A \to 0$. Because the magnitude of the wavenumber k in figure 4 is smaller than that in figure 3, the phase speed ω/k will be larger in figure 4 than in figure 3. Therefore, the wave in figure 4 is called the fast wave.

To consider the relation between k_x and k_z for a fixed frequency, we write (45) as

$$\begin{aligned}
&\cos^2\phi\, k_z^4 + \sin 2\phi\, k_x k_z^3 \\
&+\left[2k_x^2\cos^2\phi - \omega^2\left(c_s^{-2} + c_A^{-2}\right) + k_A^2\cos^2\phi - k_x^2\cos 2\phi\right] k_z^2 \\
&+k_x^3\sin 2\phi\, k_z + k_x^4\cos^2\phi \\
&+\left[-\omega^2\left(c_s^{-2} + c_A^{-2}\right) + k_A^2\cos^2\phi + N^2c_A^{-2} - k_x^2\cos 2\phi\right] k_x^2 \\
&+\left(\omega^2 - \omega_a^2\right)\omega^2/(c_A^2 c_s^2) = 0\,. \qquad (47)
\end{aligned}$$

Equation (47) can be solved as a quartic equation in k_z as a function of k_x. The result is shown in figure 5, which shows the dispersion relation relating k_x and k_z for a frequency of 0.01 Hz. The second factor in (44) shows that the approximate formula for the nearly straight lines that describe the slow magneto-acoustic wave in figures 3, 5, and 6 is

$$k_H^2 = (k_z\cos\phi + k_x\sin\phi)^2 \approx \omega^2\left(1/c_A^2 + 1/c_s^2\right) - k_A^2\cos^2\phi\,. \quad (48)$$

However, the dispersion relation for the slow magnetoacoustic

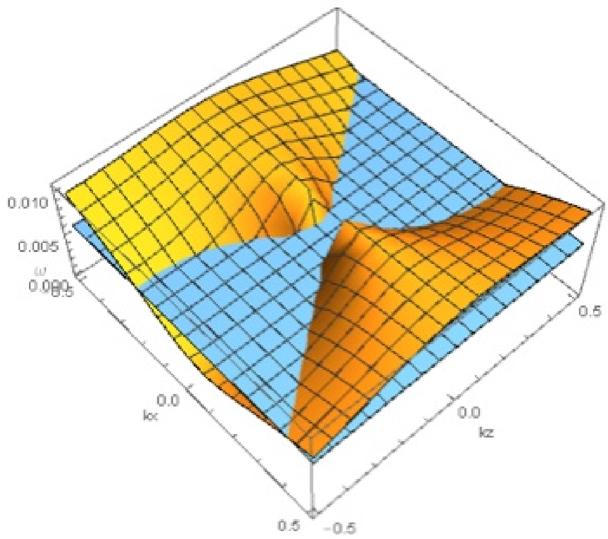

Figure 1: Dispersion relation for a magneto-acoustic-gravity wave for propagation in the same vertical plane as the Earth's magnetic field. The surface gives the intrinsic frequency in rad s^{-1} as a function of k_x and k_z in km^{-1}. Also shown is the intersection of the surface with a horizontal plane for an intrinsic frequency of 0.001 Hz, which is below the acoustic cutoff frequency for this case. The sound speed, $c_s = 0.3$ km s^{-1}. The acoustic cut-off frequency $\omega_a = 0.0105$ radians s^{-1}. The Brunt-Väisälä frequency, $N = 0.01$ s^{-1}. The angle between the magnetic field and vertical, $\phi = 45°$. The Alfvén speed, $c_A = 0.01$ km s^{-1}. The effect of the magnetic field is smaller here than it is in figure 2 because of the smaller Alfvén speed here. Generally, the effect of the magnetic field increases with height in the atmosphere as the Alfvén speed increases because it is inversely proportional the the square root of density. The value of c_A in this figure corresponds to a height of about 95 km if we use a value of 8.5 km as the density scale height (Ostrovsky, 2008). Color online.

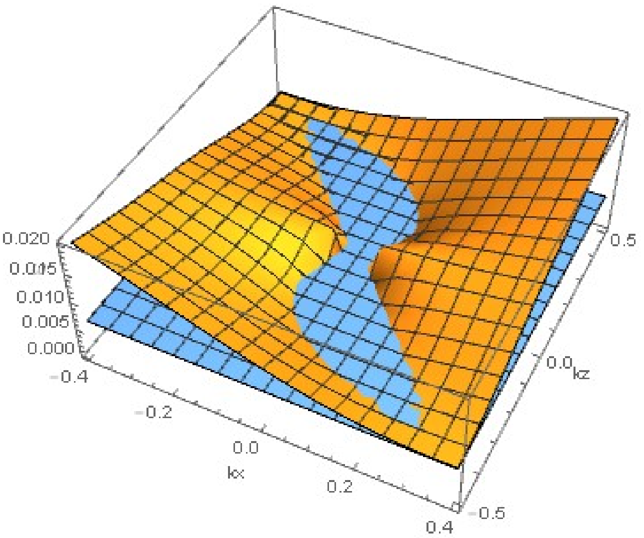

Figure 2: Dispersion relation for a magneto-acoustic-gravity wave for propagation in the same vertical plane as the Earth's magnetic field. The surface gives the intrinsic frequency in rad s^{-1} as a function of k_x and k_z in km^{-1}. Also shown is the intersection of the surface with a horizontal plane for an intrinsic frequency of 0.001 Hz, which is below the acoustic cutoff frequency for this case. The Alfvén speed, $c_A = 0.03$ km s^{-1}. Otherwise, conditions as in figure 1. The effect of the magnetic field is larger here than it is in figure 1 because of the larger Alfvén speed here. Generally, the effect of the magnetic field increases with height in the atmosphere as the Alfvén speed increases because it is inversely proportional the the square root of density. The part of the dispersion relation near the origin corresponds to a gravity wave. The part away from the origin corresponds to a magnetoacoustic wave. Where they join gives the possibility of coupling between the two kinds of waves. The value of c_A in this figure corresponds to a height of about 115 km if we use a value of 8.5 km as the density scale height (Ostrovsky, 2008). Color online.

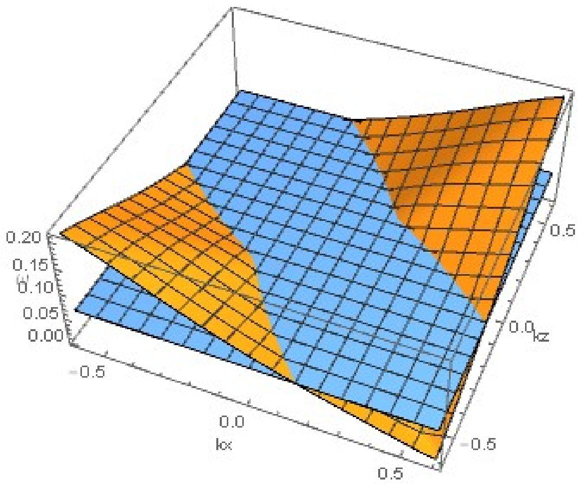

Figure 3: Dispersion relation for a slow magneto-acoustic-gravity wave for propagation in the same vertical plane as the Earth's magnetic field. The surface gives the intrinsic frequency in rad s^{-1} as a function of k_x and k_z in km^{-1}. This is a slow magnetoacoustic wave. Also shown is the intersection of the surface with a horizontal plane for an intrinsic frequency of 0.01 Hz, which is above the acoustic cutoff frequency for this case. The Alfvén speed, $c_A = 0.25$ km s^{-1}. Otherwise, conditions as in figure 1. The conditions in this figure represent the case where the Alfvén speed c_A is slightly smaller than the sound speed c_s, which would occur at a height of about 152 km in the atmosphere if we use a value of 8.5 km as the density scale height (Ostrovsky, 2008). Color online.

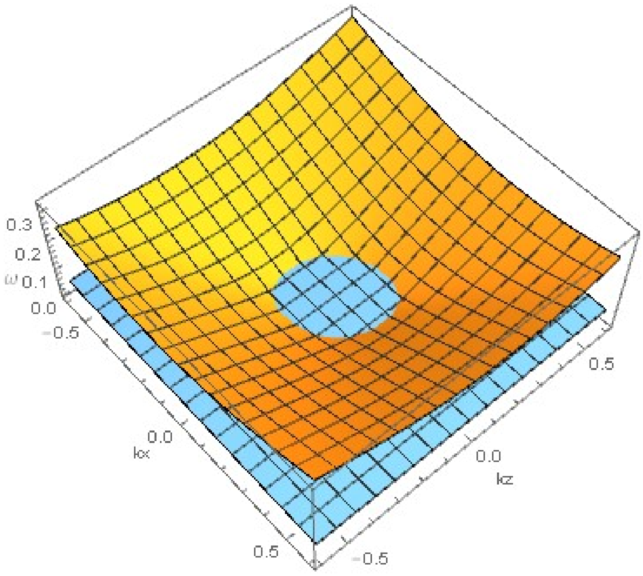

Figure 4: Dispersion relation for a fast magneto-acoustic-gravity wave for propagation in the same vertical plane as the Earth's magnetic field. The surface gives the intrinsic frequency in rad s^{-1} as a function of k_x and k_z in km^{-1}. This is a fast magnetoacoustic wave. Also shown is the intersection of the surface with a horizontal plane for an intrinsic frequency of 0.01 Hz, which is above the acoustic cutoff frequency for this case. The Alfvén speed, $c_A = 0.25$ km s^{-1}. Otherwise, conditions as in figure 1. The conditions in this figure represent the case where the Alfvén speed c_A is slightly smaller than the sound speed c_s, which would occur at a height of about 152 km in the atmosphere if we use a value of 8.5 km as the density scale height (Ostrovsky, 2008). Color online.

wave deviates more noticeably from a straight line as c_A increases.

Figure 6 shows the corresponding case for $c_A = 0.35$ km s^{-1}. In this case, with $c_A > c_s$, the center portion is magnetic sound. As (41) shows, the Alfvén speed is proportional the the magnetic field and inversely proportional to the square root of the density. Therefor, c_A will grow approximately exponentially with height because the approximately exponential decay of density with height dominates the height variation.

We can use (44) and [(65) in section 12] to analyze figures 3 through 6. Looking at (44), we see that the gravity terms that contain k_A and N are small for the values in figures 3 through 6, so that (44) reduces to (65) for the $k_y = 0$ case. We use (65) for the main analysis, but sometimes refer to (44) to see how gravity alters the main effects.

To orient ourselves, the magnetic field is in the k_x-k_z plane, at a 45° angle with the k_z axis, pointing roughly perpendicular to the two nearly straight lines in figures 3, 5, and 6. The component of $\mathbf{k}$ in the direction of the magnetic field is k_H. The square of the component of $\mathbf{k}$ in the direction normal to the magnetic field is $k^2 - k_H^2$.

From (65), we see that the magnitude of the component of $\mathbf{k}$ normal to the magnetic field will be zero when the component of $\mathbf{k}$ along the magnetic field is ω/c_s or ω/c_A. That gives four intersections of the dispersion relation function with a line through the origin that is in the direction of the magnetic field. Figures 3 and 4 each show two of those intersections, and fig-

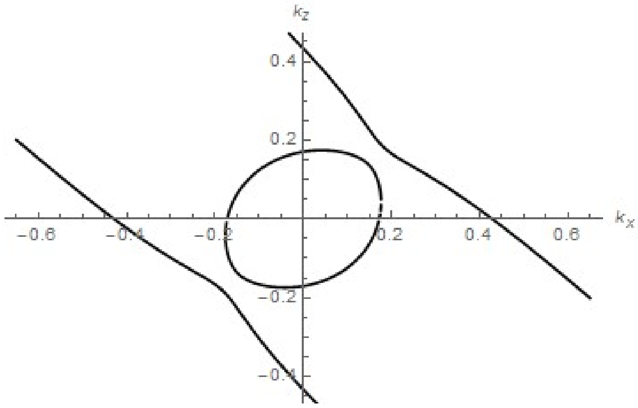

Figure 5: Dispersion relation for magneto-acoustic-gravity waves for propagation in the same vertical plane as the Earth's magnetic field for an intrinsic frequency (0.01 Hz) above the acoustic cutoff frequency. The vertical axis is k_z in km s^{-1}. The horizontal axis is k_x in km s^{-1}. The Alfvén speed, $c_A = 0.25$ km s^{-1}. Otherwise, conditions as in figure 1. The center part is a fast magnetoacoustic wave. The outer portion is a slow magnetoacoustic wave. From the lower left to the upper right, the distances from the origin are approximately: ω/c_A, ω/c_s, ω/c_s, and ω/c_A. Because of the effect of gravity, the distances are only approximate. The conditions in this figure represent the case where the Alfvén speed c_A is slightly smaller than the sound speed c_s, which would occur at a height of about 152 km in the atmosphere if we use a value of 8.5 km as the density scale height (Ostrovsky, 2008). If the Alfvén speed c_A and the sound speed c_s were equal, the two branches of the dispersion relation would touch, and there would be coupling between the acoustic waves and the magnetic sound waves. This would occur at a height of about 155 km in the atmosphere because of the exponential growth of C_A with height (Ostrovsky, 2008).

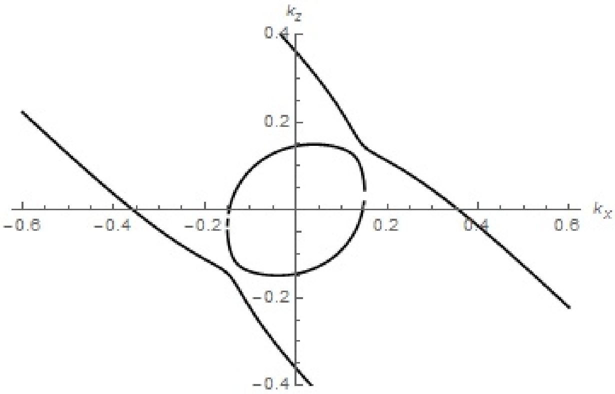

Figure 6: Dispersion relation for magneto-acoustic-gravity waves for propagation in the same vertical plane as the Earth's magnetic field for an intrinsic frequency (0.01 Hz) above the acoustic cutoff frequency. The vertical axis is k_z in km s^{-1}. The horizontal axis is k_x in km s^{-1}. The Alfvén speed, $c_A = 0.35$ km s^{-1}. Otherwise, conditions as in figure 1. The center part is a fast magnetoacoustic wave. The outer portion is a slow magnetoacoustic wave. From the lower left to the upper right, the distances from the origin are approximately: ω/c_s, ω/c_A, ω/c_A, and ω/c_s. Because of the effect of gravity, the distances are only approximate. The conditions in this figure represent the case where the Alfvén speed c_A is slightly greater than the sound speed c_s, which would occur at a height of about 158 km in the atmosphere if we use a value of 8.5 km as the density scale height (Ostrovsky, 2008). If the Alfvén speed c_A and the sound speed c_s were equal, the two branches of the dispersion relation would touch, and there would be coupling between the acoustic waves and the magnetic sound waves. This would occur at a height of about 155 km in the atmosphere because of the exponential growth of C_A with height (Ostrovsky, 2008).

ures 5 and 6 each show all four intersections. Because $c_A < c_s$ in figures 3, 4, and 5, ω/c_s will give the intersections closer to the origin in figure 5, and the only intersections in figure 4. ω/c_A will give the intersections farther from the origin in figure 5, and the only intersections in figure 3. Similarly, because $c_A > c_s$ in figure 6, ω/c_A will give the intersections closer to the origin in figure 6 and ω/c_s will give the intersections farther from the origin in figure 6. Equation (44) can be used to show that gravitational effects alter these calculations slightly.

From (65), we see that component of $\mathbf{k}$ normal to the magnetic field is infinite when the denominator on the right-hand side of (65) is zero. That allows us to calculate the asymptotic values of the nearly straight lines in figures 3, 5, and 6 as giving $k_H^2 = \omega^2/c_s^2 + \omega^2/c_A^2$. Equation (44) can be used to show that gravitational effects alter these calculations slightly.

Setting k_H to zero in (65) shows that the "radius" of the small "circle" in the direction normal to the magnetic field in figures 4, 5, and 6 is approximately $\omega/\sqrt{c_s^2 + c_A^2}$. Equation (44) can be used to show that gravitational effects alter these calculations slightly.

11.2. *In the $k_y - k_z$ plane*

For propagation in the $k_y - k_z$ plane, the dispersion relation becomes

$$\left[\omega^2 - c_A^2 k_z^2 \cos^2\phi\right]\Big\{(\omega^2 - \omega_a^2)\omega^2$$
$$+k_y^2\left[N^2 c_s^2 - \omega^2(c_s^2 + c_A^2) + c_A^2\omega_a^2\cos^2\phi + c_A^2 c_s^2 k_z^2\cos^2\phi\right]$$
$$+k_z^2\left[-\omega^2(c_s^2 + c_A^2) + c_A^2\omega_a^2\cos^2\phi + c_A^2 c_s^2 k_z^2\cos^2\phi\right]\Big\}$$

$$+k_y^2 c_A^2\omega^2\omega_a^2\sin^2\phi = 0\,. \tag{49}$$

Factoring out the Alfvén wave gives

$$\begin{aligned}&(\omega^2 - \omega_a^2)\omega^2\\ &+k_y^2\left[N^2 c_s^2 - \omega^2(c_s^2 + c_A^2) + c_A^2\omega_a^2 f_1 + c_A^2 c_s^2 k_z^2\cos^2\phi\right]\\ &+k_z^2\left[-\omega^2(c_s^2 + c_A^2) + c_A^2\omega_a^2\cos^2\phi + c_A^2 c_s^2 k_z^2\cos^2\phi\right]\\ &= 0\,,\end{aligned} \tag{50}$$

where

$$f_1 \equiv \frac{\omega^2 - c_A^2 k_z^2\cos^4\phi}{\omega^2 - c_A^2 k_z^2\cos^2\phi}\,. \tag{51}$$

The dispersion-relation curve in the $k_y - k_z$ plane intersects the k_y axis in two places, which are

$$k_y^2 = \frac{(\omega_a^2 - \omega^2)\omega^2}{N^2 c_s^2 - \omega^2(c_s^2 + c_A^2) + c_A^2\omega_a^2}\,. \tag{52}$$

The dispersion relation in the $k_y - k_z$ plane is more complicated because of the possible coupling with the Alfvén wave.

11.3. *In an arbitrary vertical plane*

For propagation in an arbitrary vertical plane that makes an angle θ with the vertical plane containing the magnetic field, the dispersion relation is

$$(\omega^2 - \omega_a^2)\omega^2$$

$$
\begin{aligned}
&+k_h^2\left[N^2c_s^2-\omega^2(c_s^2+c_A^2)+c_A^2\omega_a^2 f_2+c_A^2c_s^2k_H^2\right]\\
&+k_z^2\left[-\omega^2(c_s^2+c_A^2)+c_A^2\omega_a^2\cos^2\phi+c_A^2c_s^2k_H^2\right]\\
&=0\,,
\end{aligned} \tag{53}
$$

where the horizontal component of the wave vector is k_h,

$$
f_2 \equiv \frac{\left(\cos^2\phi+\sin^2\phi\sin^2\theta\right)\omega^2-c_A^2k_H^2\cos^2\phi}{\omega^2-c_A^2k_H^2}\,, \tag{54}
$$

and

$$
k_H^2 = k_h^2\cos^2\theta\sin^2\phi + 2k_hk_z\cos\theta\sin\phi\cos\phi + k_z^2\cos^2\phi\,. \tag{55}
$$

Equation (53) can be written as

$$
\begin{aligned}
&c_A^2c_s^2k^2k_H^2\\
&+k^2\left[-\omega^2\left(c_s^2+c_A^2\right)+c_A^2\omega_a^2\cos^2\phi\right]\\
&+\left(\omega^2-\omega_a^2\right)\omega^2+N^2c_s^2k_h^2+k_y^2\sin^2\phi\frac{c_A^2\omega^2\omega_a^2}{\omega^2-c_A^2k_H^2}\\
&=0\,.
\end{aligned} \tag{56}
$$

Or,

$$
\begin{aligned}
&c_A^2c_s^2\cos^2\phi k^4\\
&+k^2\left[-\omega^2\left(c_s^2+c_A^2\right)+c_A^2\omega_a^2\cos^2\phi\right.\\
&\left.+c_A^2c_s^2\left(2k_hk_z\cos\theta\sin\phi\cos\phi+k_h^2(\sin^2\phi\cos^2\theta-\cos^2\phi)\right)\right]\\
&+\left(\omega^2-\omega_a^2\right)\omega^2+N^2c_s^2k_h^2+k_y^2\sin^2\phi\frac{c_A^2\omega^2\omega_a^2}{\omega^2-c_A^2k_H^2}\\
&=0\,.
\end{aligned} \tag{57}
$$

It can be seen from figure 2, that magnetoacoustic waves are not restricted to be above the acoustic-cutoff frequency because figure 2 (which contains both magnetoacoustic and magnetogravity waves) is for a frequency below the acoustic cutoff frequency.

Reflection of magnetogravity waves at ionospheric heights is controlled by the rapid increase of c_A^2 with height as the density of the atmosphere decreases as seen in (41). Looking at (53), we see that as c_A^2 increases in the second term in the coefficient of k_h^2, there will be a height where the k_h^2 term no longer dominates the $(\omega^2-\omega_a^2)\omega^2$ term. At that point, k_z^2 will be zero, and would be negative above that height, indicating an evanescent region. Reflection occurs at that height.

12. Magnetoacoustic waves

To compare with previous results in the special case of a pure magnetoacoustic wave (Ostrovsky, 2008) (also called a magnetosonic wave (Landau et al., 1984)) without losses, we neglect all but the first three matrices in $\hat{\mathbf{M}}$ as given by (A.2) and in $\mathbf{M}$ as given by (B.3). That is, we take

$$
\hat{\mathbf{M}} = \hat{\mathbf{M}}_1+\hat{\mathbf{M}}_2+\hat{\mathbf{M}}_3 \tag{58}
$$

and

$$
\mathbf{M} = \mathbf{M}_1+\mathbf{M}_2+\mathbf{M}_3\,. \tag{59}
$$

Multiplying the determinant of (59) by $c_s^2H_x^2H_y^2H_z^2/((4\pi\rho)^3\omega^2)$ and setting it to zero gives[5]

$$
\begin{aligned}
&\omega^4\left(\omega^2-c_s^2k^2-\frac{(\mathbf{H}\cdot\mathbf{k})^2+H^2k^2}{4\pi\rho}\right)+\frac{H^2k^2\omega^2(\mathbf{H}\cdot\mathbf{k})^2}{(4\pi\rho)^2}\\
&+\frac{c_s^2k^2(\mathbf{H}\cdot\mathbf{k})^2}{4\pi\rho}\left[2\omega^2-\frac{(\mathbf{H}\cdot\mathbf{k})^2}{4\pi\rho}\right]=0
\end{aligned} \tag{60}
$$

for the dispersion relation. Notice that in the absence of the Earth's magnetic field, the dispersion relation reduces to the standard dispersion relation for an acoustic wave. We can factor (60) to give

$$
\left[\omega^2-\frac{(\mathbf{H}\cdot\mathbf{k})^2}{4\pi\rho}\right]\left[\omega^4-\left(c_s^2+\frac{H^2}{4\pi\rho}\right)k^2\omega^2+\frac{c_s^2(\mathbf{H}\cdot\mathbf{k})^2k^2}{4\pi\rho}\right]=0 \tag{61}
$$

for the dispersion relation. The first factor in (61),

$$
\omega^2-\frac{(\mathbf{H}\cdot\mathbf{k})^2}{4\pi\rho}=0\,, \tag{62}
$$

gives the dispersion relation for an Alfvén wave, where the group velocity is parallel to the background magnetic field and has a speed equal to the Alfvén speed, and for an arbitrary direction of the wave normal, the trace speed in the direction of the background magnetic field is also equal to the Alfvén speed.

The second factor in (61),

$$
\omega^4-\left(c_s^2+\frac{H^2}{4\pi\rho}\right)k^2\omega^2+\frac{c_s^2(\mathbf{H}\cdot\mathbf{k})^2k^2}{4\pi\rho}=0\,, \tag{63}
$$

is one form of the dispersion relation for the two magneto-acoustic waves (Ostrovsky, 2008, eq. (3)). Another form for the dispersion relation is

$$
\omega^4-\left(c_s^2+\frac{H^2}{4\pi\rho}\right)k^2\omega^2+\frac{c_s^2H^2k_H^2k^2}{4\pi\rho}=0\,, \tag{64}
$$

where k_H is the component of $\mathbf{k}$ parallel to $\mathbf{H}$. A symmetric form of the dispersion relation that is a special case of (44) is

$$
\frac{k^2-k_H^2}{\omega^2}=\frac{\left(\frac{1}{c_s^2}-\frac{k_H^2}{\omega^2}\right)\left(\frac{1}{c_A^2}-\frac{k_H^2}{\omega^2}\right)}{\frac{1}{c_s^2}+\frac{1}{c_A^2}-\frac{k_H^2}{\omega^2}}\,. \tag{65}
$$

Ostrovsky and Rubakha (1972) calculated the nonlinear effects of the propagation of a magnetoacoustic wave in the vertical direction, including the effects of the magnetic field.

13. Hamiltonian ray tracing for Magnetoacoustic waves

As mentioned above, an appropriate computer program to calculate ray paths using the dispersion relation in (64) is the general three-dimensional ray tracing program for calculating acoustic-gravity waves in the atmosphere (described in Bedard and Jones, 2013; Jones and Bedard, 2015).

In that case, we would use

$$
H(t,x_i,\sigma,k_i)=\omega^4-\left(c_s^2+\frac{H^2}{4\pi\rho}\right)k^2\omega^2+\frac{c_s^2H^2k_H^2k^2}{4\pi\rho} \tag{66}
$$

[5]as verified by an algebraic manipulation program (Mathematica)

for the Hamiltonian. To initialize a ray-path calculation, one chooses the frequency and the wave-normal direction (that is, the direction of **k**). To determine all of the components of **k**, it is necessary calculate the magnitude of **k** from the dispersion relation. If there were no background wind, then ω in (66) would equal the wave frequency and we could use the following form of the dispersion relation

$$\omega^4 - \left(c_s^2 + \frac{H^2}{4\pi\rho}\right)k^2\omega^2 + \frac{c_s^2 H_k^2 k^4}{4\pi\rho} = 0 \tag{67}$$

to determine the magnitude of **k**, where H_k is the component of **H** parallel to **k**. If, however, there is a background wind **U**, then we must use (B.1) for the intrinsic frequency in (67). That gives

$$(\sigma - \mathbf{k}\cdot\mathbf{U})^4 - \left(c_s^2 + \frac{H^2}{4\pi\rho}\right)k^2(\sigma - \mathbf{k}\cdot\mathbf{U})^2 + \frac{c_s^2 H_k^2 k^4}{4\pi\rho} = 0\,, \tag{68}$$

which will give a quartic equation to determine k.

14. Concluding remarks

Equation (B.2) gives the general magneto-acoustic-gravity-wave dispersion relation neglecting dissipation and nonlinear effects. Equation (27) gives the dispersion relation in the special case where we neglect Coriolis force, vorticity, and symmetric rate-of-strain. Equation (37) gives the dispersion relation in a current-free region. The barotropic approximation to the dispersion relation is in (38), or for a current-free region, in (40) and (42). Equation (65) gives the special case of the dispersion relation for magnetoacoustic-waves. In the absence of the magnetic field, the dispersion relation in each of the above cases reduces to that of the corresponding case for acoustic-gravity waves (Jones, 2001, 2005, 2006).

These dispersion relations can be used as a Hamiltonian to calculate ray paths in a general atmospheric ray tracing program (e.g. Bedard and Jones, 2013; Jones and Bedard, 2015; Jones et al., 1986a,b; Georges et al., 1990). Keeping all terms in the determinant-form of the dispersion relation in (B.2) will permit quantitatively assessing the significance of all of the terms[6], as well as insuring that application of the WKB approximation will be to the correct set of equations and not to an approximate set of equations.

Generalizing the dispersion relation in raytracing to include magneto-acoustic-gravity waves is useful, but using gravity waves from the ground to the ionosphere as a practical method of earthquake warning depends on having early precursors (Blaunstein and Hayakawa, 2009) because the travel time of gravity waves from the Earth surface to the ionosphere varies from hours to days (Jones and Bedard, 2016). The travel-time calculations could be tested using the full magneto-acoustic-gravity wave dispersion relation.

The dispersion relation for the special case of magneto-acoustic waves in (64) or (65) could also be used as a Hamiltonian in a ray tracing program. Because propagation of acoustic waves is so much faster than gravity waves, ray tracing of magnetoacoustic waves could provide a practical method for testing the possibility of detecting earthquake precursors by monitoring the ionosphere.

The following reference validations were done in developing these dispersion relations:

- When the effects of vorticity, rotation of the Earth, and rate of strain are neglected and the magnetic field is set to zero, the expression for magneto-acoustic-gravity waves agrees with the usual dispersion relation for acoustic-gravity waves in a baroclinic fluid.
- Magnetoacoustic wave dispersion relation - In the absence of the Earth's magnetic field, the dispersion relation reduces to the standard dispersion relation for acoustic waves.
- Magneto-acoustic-gravity wave dispersion relation - In the absence of the Earth's magnetic field, this reduces to the dispersion relation for acoustic-gravity waves.

In addition, it is of general theoretical interest to understand the propagation processes for how earthquake ground motion affects the ionosphere. Knowing the dispersion relation for magneto-acoustic-gravity waves will help in understanding how earthquake ground motion affects the ionosphere.

There is a challenge in evaluating the relative importance of various terms, but the dispersion relations presented here will make that easier to do.

There are a wealth of wave complexities and situations that can be explained using the magneto-acoustic-gravity-wave dispersion relations under varying conditions (e.g. wind profiles and temperature profiles). The dispersion relation presented here should find valuable applications.

Acknowledgments

We thank the anonymous reviewer for many useful comments and suggestions.

Appendix A. Matrix representation

We can compactly write (9), (12), (13), and (14) as a single matrix equation as

$$\hat{\mathbf{M}}\begin{pmatrix} \rho_0^{1/2}u \\ \rho_0^{1/2}v \\ \rho_0^{1/2}w \\ \rho_0^{-1/2}\delta\tilde{\rho}_{pot} \\ \rho_0^{-1/2}\delta p \\ 4\pi\rho_0^{1/2}h_x/H_{0x} \\ 4\pi\rho_0^{1/2}h_y/H_{0y} \\ 4\pi\rho_0^{1/2}h_z/H_{0z} \end{pmatrix} = -i\rho_0^{1/2}\begin{pmatrix} \delta L_{1x} \\ \delta L_{1y} \\ \delta L_{1z} \\ 0 \\ 0 \\ \delta L_{2x}/H_{0x} \\ \delta L_{2y}/H_{0y} \\ \delta L_{2z}/H_{0z} \end{pmatrix}. \tag{A.1}$$

[6] by using the determinant as the Hamiltonian in a ray-tracing program, and comparing ray-path calculations with and without various terms

From here on, we neglect the dissipation terms, $\mathbf{L}_1$ and $\mathbf{L}_2$, but there may be situations where the dissipation terms are significant (e.g. Hickey and Cole, 1987).

The first three rows in (A.1) are the components of the linearized momentum equations (9). The fourth row is the linearized adiabatic condition (13). The fifth row is the difference between the linearized continuity equation (12) and the linearized adiabatic condition (13). The last three rows are the linearized equations for the Earth's magnetic field (14). The matrix $\hat{\mathbf{M}}$ is the 8×8 matrix given by

$$\hat{\mathbf{M}} = \sum_{i=1}^{3} \hat{\mathbf{M}}_i + \sum_{i=4}^{12} + \mathbf{M}_i \,, \tag{A.2}$$

and the various matrices above are defined as follows.

$$\hat{\mathbf{M}}_1 = -\begin{pmatrix} 1 & 0 & 0 & 0 & 0 & 0 & 0 & 0 \\ 0 & 1 & 0 & 0 & 0 & 0 & 0 & 0 \\ 0 & 0 & 1 & 0 & 0 & 0 & 0 & 0 \\ 0 & 0 & 0 & 1 & 0 & 0 & 0 & 0 \\ 0 & 0 & 0 & 0 & \frac{1}{c_s^2} & 0 & 0 & 0 \\ 0 & 0 & 0 & 0 & 0 & \frac{4\pi\rho}{H_x^2} & 0 & 0 \\ 0 & 0 & 0 & 0 & 0 & 0 & \frac{4\pi\rho}{H_y^2} & 0 \\ 0 & 0 & 0 & 0 & 0 & 0 & 0 & \frac{4\pi\rho}{H_z^2} \end{pmatrix} \hat{\omega} \,, \tag{A.3}$$

where $\hat{\omega} \equiv iD_0/Dt = \partial/\partial t + \mathbf{U_0} \cdot \nabla$, and zero subscripts have been dropped from the matrices for compactness. All quantities within matrices (except the differential operators $\hat{\omega}$ and $\hat{\mathbf{k}}$) are background quantities.

$$\hat{\mathbf{M}}_2 = \begin{pmatrix} 0 & 0 & 0 & 0 & \hat{k}_x & \hat{k}_x & \hat{k}_x & \hat{k}_x \\ 0 & 0 & 0 & 0 & \hat{k}_y & \hat{k}_y & \hat{k}_y & \hat{k}_y \\ 0 & 0 & 0 & 0 & \hat{k}_z & \hat{k}_z & \hat{k}_z & \hat{k}_z \\ 0 & 0 & 0 & 0 & 0 & 0 & 0 & 0 \\ \hat{k}_x & \hat{k}_y & \hat{k}_z & 0 & 0 & 0 & 0 & 0 \\ \hat{k}_x & \hat{k}_y & \hat{k}_z & 0 & 0 & 0 & 0 & 0 \\ \hat{k}_x & \hat{k}_y & \hat{k}_z & 0 & 0 & 0 & 0 & 0 \\ \hat{k}_x & \hat{k}_y & \hat{k}_z & 0 & 0 & 0 & 0 & 0 \end{pmatrix} , \tag{A.4}$$

$\hat{\mathbf{k}} \equiv -i\nabla$,

$$\hat{\mathbf{M}}_3 = -\begin{pmatrix} 0 & 0 & 0 & 0 & 0 & \frac{1}{H_x} & 0 & 0 \\ 0 & 0 & 0 & 0 & 0 & 0 & \frac{1}{H_y} & 0 \\ 0 & 0 & 0 & 0 & 0 & 0 & 0 & \frac{1}{H_z} \\ 0 & 0 & 0 & 0 & 0 & 0 & 0 & 0 \\ 0 & 0 & 0 & 0 & 0 & 0 & 0 & 0 \\ \frac{1}{H_x} & 0 & 0 & 0 & 0 & 0 & 0 & 0 \\ 0 & \frac{1}{H_y} & 0 & 0 & 0 & 0 & 0 & 0 \\ 0 & 0 & \frac{1}{H_z} & 0 & 0 & 0 & 0 & 0 \end{pmatrix} \mathbf{H}\cdot\hat{\mathbf{k}} \,, \tag{A.5}$$

$$\mathbf{M}_4 = \begin{pmatrix} 0 & 2i\tilde{\Omega}_z & -2i\tilde{\Omega}_y & 0 & 0 & 0 & 0 & 0 \\ -2i\tilde{\Omega}_z & 0 & 2i\tilde{\Omega}_x & 0 & 0 & 0 & 0 & 0 \\ 2i\tilde{\Omega}_y & -2i\tilde{\Omega}_x & 0 & 0 & 0 & 0 & 0 & 0 \\ 0 & 0 & 0 & 0 & 0 & 0 & 0 & 0 \\ 0 & 0 & 0 & 0 & 0 & 0 & 0 & 0 \\ 0 & 0 & 0 & 0 & 0 & 0 & 0 & 0 \\ 0 & 0 & 0 & 0 & 0 & 0 & 0 & 0 \\ 0 & 0 & 0 & 0 & 0 & 0 & 0 & 0 \end{pmatrix} , \tag{A.6}$$

where $\tilde{\mathbf{\Omega}} \equiv \zeta/4$, and $\zeta \equiv \nabla \times \mathbf{U}$ is the vorticity. However, if we had included Coriolis force due to the rotation of the Earth in the momentum equation (1), then we would have $\tilde{\mathbf{\Omega}} \equiv \mathbf{\Omega} + \zeta/4$, where $\mathbf{\Omega}$ is the Earth's angular velocity.

$$\mathbf{M}_5 = \frac{1}{\rho}\frac{D\rho}{Dt}\begin{pmatrix} \frac{i}{2} & 0 & 0 & 0 & 0 & 0 & 0 & 0 \\ 0 & \frac{i}{2} & 0 & 0 & 0 & 0 & 0 & 0 \\ 0 & 0 & \frac{i}{2} & 0 & 0 & 0 & 0 & 0 \\ 0 & 0 & 0 & -\frac{i}{2} & 0 & 0 & 0 & 0 \\ 0 & 0 & 0 & i & \frac{i\rho^{1/2}}{c_s^4}\left(\frac{\partial\rho^{1/2}c_s^2}{\partial\rho}\right)_{sS} & 0 & 0 & 0 \\ 0 & 0 & 0 & 0 & 0 & 0 & 0 & 0 \\ 0 & 0 & 0 & 0 & 0 & 0 & 0 & 0 \\ 0 & 0 & 0 & 0 & 0 & 0 & 0 & 0 \end{pmatrix} , \tag{A.7}$$

where the partial derivative in (A.7) is with holding the entropy and the chemical composition constant,

$$\mathbf{M}_6 = \begin{pmatrix} 0 & 0 & 0 & i\tilde{g}_x & -i\tilde{\Gamma}_x & 0 & 0 & 0 \\ 0 & 0 & 0 & i\tilde{g}_y & -i\tilde{\Gamma}_y & 0 & 0 & 0 \\ 0 & 0 & 0 & i\tilde{g}_z & -i\tilde{\Gamma}_z & 0 & 0 & 0 \\ -ik_{Bx} & -ik_{By} & -ik_{Bz} & 0 & 0 & 0 & 0 & 0 \\ i\Gamma_x & i\Gamma_y & i\Gamma_z & 0 & 0 & 0 & 0 & 0 \\ 0 & 0 & 0 & 0 & 0 & 0 & 0 & 0 \\ 0 & 0 & 0 & 0 & 0 & 0 & 0 & 0 \\ 0 & 0 & 0 & 0 & 0 & 0 & 0 & 0 \end{pmatrix} , \tag{A.8}$$

$\mathbf{k}_A \equiv \nabla\rho/(2\rho)$, $\mathbf{k}_B \equiv \nabla\tilde{\rho}_{\mathrm{pot}}/\rho$,

$$\mathbf{M}_7 = \frac{i}{2\rho}\begin{pmatrix} -ie_{xx} & -ie_{xy} & -ie_{xz} & 0 & 0 & -\frac{\partial\rho}{\partial x} & -\frac{\partial\rho}{\partial x} & -\frac{\partial\rho}{\partial x} \\ -ie_{yx} & -ie_{yy} & -ie_{yz} & 0 & 0 & -\frac{\partial\rho}{\partial y} & -\frac{\partial\rho}{\partial y} & -\frac{\partial\rho}{\partial y} \\ -ie_{zx} & -ie_{zy} & -ie_{zz} & 0 & 0 & -\frac{\partial\rho}{\partial z} & -\frac{\partial\rho}{\partial z} & -\frac{\partial\rho}{\partial z} \\ 0 & 0 & 0 & 0 & 0 & 0 & 0 & 0 \\ 0 & 0 & 0 & 0 & 0 & 0 & 0 & 0 \\ \frac{\partial\rho}{\partial x} & \frac{\partial\rho}{\partial y} & \frac{\partial\rho}{\partial z} & 0 & 0 & 0 & 0 & 0 \\ \frac{\partial\rho}{\partial x} & \frac{\partial\rho}{\partial y} & \frac{\partial\rho}{\partial z} & 0 & 0 & 0 & 0 & 0 \\ \frac{\partial\rho}{\partial x} & \frac{\partial\rho}{\partial y} & \frac{\partial\rho}{\partial z} & 0 & 0 & 0 & 0 & 0 \end{pmatrix} , \tag{A.9}$$

and $\mathbf{e}$ is the matrix representing the symmetric rate-of-strain tensor (Aris, 1962, p. 89), (Cole, 1962, p. 228), (Monin and Yaglom, 1987), whose components are

$$e_{ij} \equiv \frac{1}{2}\left(\frac{\partial U_i}{\partial x_j} + \frac{\partial U_j}{\partial x_i}\right) , \tag{A.10}$$

$$\mathbf{M}_8 = \frac{i\mathbf{H}\cdot\nabla\rho}{2\rho}\begin{pmatrix} 0 & 0 & 0 & 0 & 0 & \frac{1}{H_x} & 0 & 0 \\ 0 & 0 & 0 & 0 & 0 & 0 & \frac{1}{H_y} & 0 \\ 0 & 0 & 0 & 0 & 0 & 0 & 0 & \frac{1}{H_z} \\ 0 & 0 & 0 & 0 & 0 & 0 & 0 & 0 \\ 0 & 0 & 0 & 0 & 0 & 0 & 0 & 0 \\ -\frac{1}{H_x} & 0 & 0 & 0 & 0 & 0 & 0 & 0 \\ 0 & -\frac{1}{H_y} & 0 & 0 & 0 & 0 & 0 & 0 \\ 0 & 0 & -\frac{1}{H_z} & 0 & 0 & 0 & 0 & 0 \end{pmatrix} , \tag{A.11}$$

$$\mathbf{M}_9 = i\mathbf{H}\cdot\nabla \begin{pmatrix} 0 & 0 & 0 & 0 & 0 & \frac{1}{H_x} & 0 & 0 \\ 0 & 0 & 0 & 0 & 0 & 0 & \frac{1}{H_y} & 0 \\ 0 & 0 & 0 & 0 & 0 & 0 & 0 & \frac{1}{H_z} \\ 0 & 0 & 0 & 0 & 0 & 0 & 0 & 0 \\ 0 & 0 & 0 & 0 & 0 & 0 & 0 & 0 \\ 0 & 0 & 0 & 0 & 0 & 0 & 0 & 0 \\ 0 & 0 & 0 & 0 & 0 & 0 & 0 & 0 \\ 0 & 0 & 0 & 0 & 0 & 0 & 0 & 0 \end{pmatrix} , \tag{A.12}$$

$$\mathbf{M}_{10} = \begin{pmatrix} 0 & 0 & 0 & 0 & 0 & \frac{1}{H_x}\frac{\partial H_x}{\partial x} & \frac{1}{H_y}\frac{\partial H_x}{\partial y} & \frac{1}{H_z}\frac{\partial H_x}{\partial z} \\ 0 & 0 & 0 & 0 & 0 & \frac{1}{H_x}\frac{\partial H_y}{\partial x} & \frac{1}{H_y}\frac{\partial H_y}{\partial y} & \frac{1}{H_z}\frac{\partial H_y}{\partial z} \\ 0 & 0 & 0 & 0 & 0 & \frac{1}{H_x}\frac{\partial H_z}{\partial x} & \frac{1}{H_y}\frac{\partial H_z}{\partial y} & \frac{1}{H_z}\frac{\partial H_z}{\partial z} \\ 0 & 0 & 0 & 0 & 0 & 0 & 0 & 0 \\ 0 & 0 & 0 & 0 & 0 & 0 & 0 & 0 \\ -\frac{1}{H_x}\frac{\partial H_x}{\partial x} & -\frac{1}{H_x}\frac{\partial H_x}{\partial y} & -\frac{1}{H_x}\frac{\partial H_x}{\partial z} & 0 & 0 & 0 & 0 & 0 \\ -\frac{1}{H_y}\frac{\partial H_y}{\partial x} & -\frac{1}{H_y}\frac{\partial H_y}{\partial y} & -\frac{1}{H_y}\frac{\partial H_y}{\partial z} & 0 & 0 & 0 & 0 & 0 \\ -\frac{1}{H_z}\frac{\partial H_z}{\partial x} & -\frac{1}{H_z}\frac{\partial H_z}{\partial y} & -\frac{1}{H_z}\frac{\partial H_z}{\partial z} & 0 & 0 & 0 & 0 & 0 \end{pmatrix} \tag{A.13}$$

$$\mathbf{M}_{11} = 4\pi i\rho \begin{pmatrix} 0 & 0 & 0 & 0 & 0 & 0 & 0 & 0 \\ 0 & 0 & 0 & 0 & 0 & 0 & 0 & 0 \\ 0 & 0 & 0 & 0 & 0 & 0 & 0 & 0 \\ 0 & 0 & 0 & 0 & 0 & 0 & 0 & 0 \\ 0 & 0 & 0 & 0 & 0 & 0 & 0 & 0 \\ 0 & 0 & 0 & 0 & 0 & \frac{1}{H_x^2}\frac{\partial U_x}{\partial x} & \frac{1}{H_xH_y}\frac{\partial U_x}{\partial y} & \frac{1}{H_xH_z}\frac{\partial U_x}{\partial z} \\ 0 & 0 & 0 & 0 & 0 & \frac{1}{H_xH_y}\frac{\partial U_y}{\partial x} & \frac{1}{H_y^2}\frac{\partial U_y}{\partial y} & \frac{1}{H_zH_y}\frac{\partial U_y}{\partial z} \\ 0 & 0 & 0 & 0 & 0 & \frac{1}{H_xH_z}\frac{\partial U_z}{\partial x} & \frac{1}{H_yH_z}\frac{\partial U_z}{\partial y} & \frac{1}{H_z^2}\frac{\partial U_z}{\partial z} \end{pmatrix} \tag{A.14}$$

$$\mathbf{M}_{12} = 2\pi i\rho_0\left(\frac{1}{\rho_0}\frac{D_0\rho_0}{Dt} - \frac{D_0}{Dt}\right)\mathbf{M}_{13} , \tag{A.15}$$

where we have used the continuity equation (2), and

$$\mathbf{M}_{13} \equiv \begin{pmatrix} 0 & 0 & 0 & 0 & 0 & 0 & 0 & 0 \\ 0 & 0 & 0 & 0 & 0 & 0 & 0 & 0 \\ 0 & 0 & 0 & 0 & 0 & 0 & 0 & 0 \\ 0 & 0 & 0 & 0 & 0 & 0 & 0 & 0 \\ 0 & 0 & 0 & 0 & 0 & 0 & 0 & 0 \\ 0 & 0 & 0 & 0 & 0 & \frac{1}{H_x^2} & 0 & 0 \\ 0 & 0 & 0 & 0 & 0 & 0 & \frac{1}{H_y^2} & 0 \\ 0 & 0 & 0 & 0 & 0 & 0 & 0 & \frac{1}{H_z^2} \end{pmatrix} . \tag{A.16}$$

That the matrices containing differential operators, $\hat{\mathbf{M}}_1$, $\hat{\mathbf{M}}_2$, and $\hat{\mathbf{M}}_3$, in (A.3), (A.4), (A.5), are symmetric exhibits explicitly that the equations (A.1) are symmetric hyperbolic, which implies that Cauchy data will be propagated causally (Courant and Hilbert, 1962; Garabedian, 1964).

Appendix B. Dispersion Relation

The dispersion relation corresponding to the differential equation (A.1) is found by following the procedure in the eikonal method (Weinberg, 1962), in which we replace the differential operator $\hat{\omega}$ by the intrinsic frequency

$$\omega = \sigma - \mathbf{k}\cdot\mathbf{U}_0 \tag{B.1}$$

(where σ is the wave frequency), replace the differential operator $\hat{\mathbf{k}}$ by the wavenumber $\mathbf{k}$, and set the determinant of $\mathbf{M}$ (possibly with some useful factors) to zero.

For the situation here, to avoid extraneous factors of density, frequency, sound speed, and components of the magnetic field, it is useful to use

$$c_s^2 H_x^2 H_y^2 H_z^2 \left|\mathbf{M}\right| / ((4\pi\rho)^3\omega^2) = 0 \tag{B.2}$$

for the dispersion relation, where

$$\mathbf{M} = \sum_{i=1}^{12} \mathbf{M}_i , \tag{B.3}$$

$$\mathbf{M}_1 = -\begin{pmatrix} 1 & 0 & 0 & 0 & 0 & 0 & 0 & 0 \\ 0 & 1 & 0 & 0 & 0 & 0 & 0 & 0 \\ 0 & 0 & 1 & 0 & 0 & 0 & 0 & 0 \\ 0 & 0 & 0 & 1 & 0 & 0 & 0 & 0 \\ 0 & 0 & 0 & 0 & \frac{1}{c_s^2} & 0 & 0 & 0 \\ 0 & 0 & 0 & 0 & 0 & \frac{4\pi\rho}{H_x^2} & 0 & 0 \\ 0 & 0 & 0 & 0 & 0 & 0 & \frac{4\pi\rho}{H_y^2} & 0 \\ 0 & 0 & 0 & 0 & 0 & 0 & 0 & \frac{4\pi\rho}{H_z^2} \end{pmatrix} \omega , \tag{B.4}$$

$$\mathbf{M}_2 = \begin{pmatrix} 0 & 0 & 0 & 0 & k_x & k_x & k_x & k_x \\ 0 & 0 & 0 & 0 & k_y & k_y & k_y & k_y \\ 0 & 0 & 0 & 0 & k_z & k_z & k_z & k_z \\ 0 & 0 & 0 & 0 & 0 & 0 & 0 & 0 \\ k_x & k_y & k_z & 0 & 0 & 0 & 0 & 0 \\ k_x & k_y & k_z & 0 & 0 & 0 & 0 & 0 \\ k_x & k_y & k_z & 0 & 0 & 0 & 0 & 0 \\ k_x & k_y & k_z & 0 & 0 & 0 & 0 & 0 \end{pmatrix} , \tag{B.5}$$

and

$$\mathbf{M}_3 = -\begin{pmatrix} 0 & 0 & 0 & 0 & 0 & \frac{1}{H_x} & 0 & 0 \\ 0 & 0 & 0 & 0 & 0 & 0 & \frac{1}{H_y} & 0 \\ 0 & 0 & 0 & 0 & 0 & 0 & 0 & \frac{1}{H_z} \\ 0 & 0 & 0 & 0 & 0 & 0 & 0 & 0 \\ 0 & 0 & 0 & 0 & 0 & 0 & 0 & 0 \\ \frac{1}{H_x} & 0 & 0 & 0 & 0 & 0 & 0 & 0 \\ 0 & \frac{1}{H_y} & 0 & 0 & 0 & 0 & 0 & 0 \\ 0 & 0 & \frac{1}{H_z} & 0 & 0 & 0 & 0 & 0 \end{pmatrix} \mathbf{H}_0\cdot\mathbf{k} . \tag{B.6}$$

The dispersion relation in (B.2) can be considered to be the general dispersion relation for a magneto-acoustic-gravity wave. In the absence of the magnetic field, the dispersion relation reduces to that for acoustic-gravity waves (Jones, 2001, 2005, 2006).

The magnetic field terms in the matrices $\mathbf{M}_8$, $\mathbf{M}_9$, $\mathbf{M}_{10}$, $\mathbf{M}_{11}$, and $\mathbf{M}_{12}$ are not usually kept in the dispersion relation for magnetoacoustic waves, but we keep those terms here in the general dispersion relation in (B.2) so that their effect can be tested by using the general dispersion relation as the Hamiltonian in a ray-tracing program, and comparing ray-path calculations with and without various terms. Similarly, the atmospheric terms in the matrix $\mathbf{M}_5$ are not usually kept in the dispersion relation for acoustic-gravity waves, but we keep those terms here in the general dispersion relation in (B.2) so that their effect can be tested.

References

Andrews, D., April 2009. Eliassen-Palm, Charney-Drazin, and the development of wave, mean-flow interaction theories in atmospheric dynamics, http://wtk.gfd-dennou.org/2009-04-06/andrews/pub/slide_2009-04-09_EP_CD.pdf (date last viewed 24 January 2017).

Andrews, D. G., McIntyre, M. E., 1976. Planetary waves in horizontal and vertical shear: the generalized eliassen-palm relation and mean zonal acceleration. J. Atmos. Sci. 33 (11), 2031–2048.

Andrews, D. G., McIntyre, M. E., 1978. Generalized Eliassen-Palm and Charney-Drazin theorems for waves on axisymmetric mean flows in compressible atmospheres. J. Atmos. Sci. 35, 175–185.

Arai, N., Iwakuni, M., Watada, S., Imanishi, Y., Murayanna, T., Imanishi, M., 2011. Atmospheric boundary layer waves excited by the tsunami generation related to the great tohoku-oki earthquake. Geophys. Res. Lett. 38, L00G18.

Aris, R., 1962. Vectors, Tensors, and the Basic Equations of Fluid Mechanics. Prentice-Hall, Inc., Englewood Cliffs, N.J.

Artru, J., Ducic, V., Kamamori, H., Lognonne, P., Murakami, M., 2005. Ionospheric detection of gravity waves induced by tsunamis. Geophys. J. Int. 160, 840–848.

Banister, J. R., Hereford, W. V., 1991. Observed high-altitude pressure waves from an underground and surface explosion. J. Geophys. Res. 96, 5185–5193, doi: 10.1029/90JD02640.

Bedard, Jr., A. J., 1971. Seismic response of infrasonic microphones. J. Res. NBS-C, Engr. and Instrum. 75C (1), 41–45.

Bedard, Jr., A. J., Jones, R. M., 2013. Infrasonic ray tracing applied to mesoscale atmospheric structures: Refraction by hurricanes. J. Acoust. Soc. Am. 134 (5), 3446–3451.

Blaunstein, N., Hayakawa, M., 2009. Short-term ionospheric precursors of earthquakes using vertical and oblique ionosondes. Physics and Chemistry of the Earth 34, 496–507.

Brillouin, L., 1926. La mécanique ondulatoire de Schrödinger; une méthode générale de résolution par approximations successives. Academie des sciences, Paris 183, 24–26.

Charney, J. G., Drazin, P. G., 1961. Propagation of planetary-scale disturbances from the lower into the upper atmosphere. Journal of Geophysical Research 66 (1), 83–109.
URL http://dx.doi.org/10.1029/JZ066i001p00083

Cole, G. H., 1962. Fluid Dynamics. Clarke, Chapman & Co. Ltd, Gateshead.

Cook, R., 1965. Radiation of sound by earthquakes. In: Proceedings 5th Interrnational Congress of Acoustics. 5th Interrnational Congress of Acoustics, Liege 7-14 Sept 1965, paper K19.

Courant, R., Hilbert, D., 1962. Methods of Mathematical Physics. Vol. 2. John Wiley and Sons, New York.

Eckart, C., 1960. Hydrodynamics of Oceans and Atmospheres. Pergamon Press, Oxford.

Einaudi, F., Hines, C. O., 1970. WKB approximation in application to acoustic-gravity waves. Can. J. Phys. 48, 1458–1471.

Eliassen, L. S., Palm, E., 1960. On the transfer of energy in stationary mountain waves. Geofysiske Publikasjoner 22 (3), 1–23.

Freund, F. T., 2003. Rocks that crackle and sparkle and glow: strange pre-earthquake phenomena. Journal of Scientific Exploration 17 (1), 37–71.
URL http://www.isfep.com/FF_EQ_SSE_2003.pdf

Garabedian, P. R., 1964. Partial Differential Equations. John Wiley & Sons, New York.

Geller, R. J., 1996. Debate on evaluation of the VAN Method: Editor's introduction. Geophys. Res. Lett. 23 (11), 1291–1293.
URL http://dx.doi.org/10.1029/96GL00742

Georges, T., 1967. Ionospheric effects of atmospheric waves. ESSA Technical Report IER 57-ITSA 54, Environmental Science Services Administration and Institute for Telecommunication Sciences and Aeronomy, 341 pp.

Georges, T. M., Jones, R. M., Lawrence, R. S., 1990. A PC version of the HARPO ocean acoustic ray-tracing program. Tech. Memo ERL WPL-180, Natl. Oceanic and Atmos. Admin., Boulder, Colorado, 18 pp. (program available at http://cires.colorado.edu/~mjones/raytracing/programs.htm).

Godin, O. A., 2015. Wentzel-Kramers-Brillouin approximation for atmospheric waves. J. Fluid Mech. 777, 260–290.

Gossard, E. E., Hooke, W. H., 1975. Waves in the Atmosphere. Elsevier Scientific Publishing Company, Amsterdam.

Heki, K., 2011. Ionospheric electron enhancement preceding the 2011 Tohoku-Oki earthquake. Geophys. Res. Lett. 38 (17).

Hickey, M., Cole, K., 1987. A quartic dispersion equation for internal gravity waves in the thermosphere. Journal of Atmospheric and Terrestrial Physics 49 (9), 889 – 899, http://dx.doi.org/10.1016/0021-9169(87)90003-1.

Hickey, M. P., 2011. Atmospheric gravity waves and effects in the upper atmosphere associated with tsunamis. In: Mörner, N.-A. (Ed.), The Tsunami Threat - Research and Technology, 2nd Edition. InTech, orders@intechopen.com, chapter 32, pp. 667–690.

Hines, C. O., 1951a. Wave packets, the poynting vector, and energy flow: 1. non-dissipative (anisotropic) homogeneous media. Journal of Geophysical Research 56 (1), 63–72.
URL http://dx.doi.org/10.1029/JZ056i001p00063

Hines, C. O., 1951b. Wave packets, the poynting vector, and energy flow: 2. group propagation through dissipative isotropic media. Journal of Geophysical Research 56 (2), 197–206.
URL http://dx.doi.org/10.1029/JZ056i002p00197

Hines, C. O., 1972. Gravity waves in the atmosphere. Nature 239, 73–78.

Jeffreys, H., 1923. On certain approximate solutions of linear differential equations of the second order. Proc. London, Math. Soc. Ser. 2 23, 428–436.

Jones, R. M., 1970. Ray theory for lossy media. Radio Science 5 (5), 793–801.
URL http://dx.doi.org/10.1029/RS005i005p00793

Jones, R. M., 1981. The frequency shift of a pulse by a time independent, dispersive, lossy medium. Tech. Memo ERL WPL-80, Natl. Oceanic and Atmos. Admin., PB8211977, 19 pp.

Jones, R. M., 1996. Three dimensional ray tracing in the atmosphere. In: W. Dieminger, G. Hartmann, R. Leitinger (Eds.), THE UPPER ATMOSPHERE. Springer Verlag, Berlin-Heidelberg, chapter II.3.1.4 (pp. 307-327) in "The Upper Atmosphere", W. Dieminger, G. Hartmann, and R. Leitinger, editors, 1014 pp., errata available at (Jones, 2007, http://cires.colorado.edu/~mjones/pubs/errata2.htm, date last viewed 26 February 2015).

Jones, R. M., 2001. The dispersion relation for internal acoustic-gravity waves in a baroclinic fluid. Physics of Fluids 13, 1274–1280, errata available at (Jones, 2012, http://cires.colorado.edu/~mjones/pubs/errata9.pdf, date last viewed 13 May 2016).

Jones, R. M., November 2005. A general dispersion relation for internal gravity waves in the atmosphere or ocean, including baroclinicity, vorticity, and rate of strain. J. Geophys. Res. 110, D22106, doi: 10.1029/2004JD005654, Errata available at (Jones, 2008a, http://cires.colorado.edu/~mjones/pubs/errata7.pdf, date last viewed 13 May 2016).

Jones, R. M., November 2006. Minimum and maximum propagation frequencies for internal gravity waves. J. Geophys. Res. 111, D06109, doi: 10.1029/2005JD006189, Errata available at (Jones, 2008b, http://cires.colorado.edu/~mjones/pubs/errata8.pdf, date last viewed 13 May 2016).

Jones, R. M., 2007. Errata: Three dimensional ray tracing in the atmosphere, pp. 307-327 in THE UPPER ATMOSPHERE, editors W. Dieminger, G. Hartmann, and R. Leitinger, springer verlag, berlin-heidelberg 1996, 1014 pages., errata available at http://cires.colorado.edu/~mjones/pubs/errata2.htm (date last viewed 26 February 2015).

Jones, R. M., 2008a. Errata: A general dispersion relation for internal gravity waves in the atmosphere or ocean, including baroclinicity, vorticity, and rate of strain, *J. Geophys. Res.*, 2005, doi: 10.1029/2004JD005654, Errata available at http://cires.colorado.edu/~mjones/pubs/errata7.pdf (date last viewed 13 May 2016).

Jones, R. M., 2008b. Errata: Minimum and maximum propagation frequencies for internal gravity waves, *J. Geophys. Res.*, 2006, doi: 10.1029/2005JD006189, Errata available at http://cires.colorado.edu/~mjones/pubs/errata8.pdf (date last viewed 13 May 2016).

Jones, R. M., 2012. Errata: The dispersion relation for internal acoustic-gravity waves in a baroclinic fluid, *Physics of Fluids*, 2001, 1274-1280, Errata available at http://cires.colorado.edu/∼mjones/pubs/errata9.pdf (date last viewed 13 May 2016).

Jones, R. M., Bedard, Jr., A. J., 2015. Infrasonic ray tracing applied to small-scale atmospheric structures: Thermal plumes and updrafts/downdrafts. J. Acoust. Soc. Am. 137 (2), 625–632.

Jones, R. M., Bedard, Jr., A. J., 2016. Acoustic-gravity-wave ray tracing. J. Geophys. Res., to be submitted December 2016.
URL http://cires.colorado.edu/$\sim$mjones/raytracing/Pub\discretionary{-}{}{}lish/GravityWavesJGR/gravity1JGR.pdf

Jones, R. M., Riley, J. P., Georges, T. M., 1986a. HARPA - A versatile three-dimensional Hamiltonian ray-tracing program for acoustic waves in the atmosphere above irregular terrain. NOAA Special Report, GovDoc No. C55.602:H 18; GPO Item No. 207-C-1; PB87132031, National Oceanic and Atmospheric Administration, Boulder, Colorado, 410 pp., report available at http://cires.colorado.edu/∼mjones/pubs/harpa.pdf (date last viewed 25 July 2016), program available at http://cires.colorado.edu/∼mjones/raytracing (date last viewed 25 July 2016).

Jones, R. M., Riley, J. P., Georges, T. M., 1986b. HARPO - A versatile three-dimensional Hamiltonian ray-tracing program for acoustic waves in an ocean with irregular bottom. NOAA Special Report, GovDoc No. C55.602:H 23; GPO Item No. 0207-C-01; PB87172573, National Oceanic and Atmospheric Administration, Boulder, Colorado, 455 pp., report available at http://cires.colorado.edu/∼mjones/pubs/harpo.pdf (date last viewed 25 July 2016), program available at http://cires.colorado.edu/∼mjones/raytracing (date last viewed 25 July 2016).

Koshevaya, S. V., Grimalsky, V. V., Burlak, G. N., Enrquez, R. P., Kotsarenko, A. N., 2001. Magnetic perturbations excited by seismic waves. Physica Scripta 64 (2), 172.
URL http://stacks.iop.org/1402-4896/64/i=2/a=016

Kramers, H. A., 1926. Wellenmechanik und halbzahlige Quantisierung. Z. Phys. 39, 828–840.

Krasnov, V. M., Drobzheva, Y. V., Chum, J., 2011. Infrasonic waves in the ionosphere generated by a weak earthquake. J. Atmos. Sol. Terr. Phys. 73, 19301939, doi: 10.1016/j.jastp.2011.05.002.

Landau, L. D., Lifshitz, E. M., Pitaevskii, L. P., 1984. Electrodynamics of continuous media, 2nd Edition. Elsevier Scientific Publishing Company, Amsterdam, volume 8 of ''Courses of Theoretical Physics".

Le Pichon, A., Guilbert, J., Vega, A., Garcés, M., Brachet, N., 2002. Ground-coupled air waves and diffracted infrasound from the arequipa earthquake of june 23 2001. Geophys. Res. Lett. 29 (18), 1886.

Le Pichon, A., Herry, P., Mialle, P., Vergoz, J., Brachet, N., Garcés, M., Drobe, D., Ceranna, L., 2005. Infrasound associated with 20042005 large sumatra earthquakes and tsunami. Geophys. Res. Lett. 32 (19), L19802.

Liouville, J., 1836. Sur le développement des fonctions ou parties de fonctions en séries dont les divers termes sont assujettis à satisfaire à une même équation différentielle du second ordre contenant un paramètre variable, I. J. Math. Pur Appl. 1, 253–265.

Liouville, J., 1837a. Sur le développement des fonctions ou parties de fonctions en séries dont les divers termes sont assujettis à satisfaire à une même équation différentielle du second ordre contenant un paramètre variable, II. J. Math. Pur Appl. 2, 16–35.

Liouville, J., 1837b. Sur le développement des fonctions ou parties de fonctions en séries dont les divers termes sont assujettis à satisfaire à une même équation différentielle du second ordre contenant un paramètre variable, III. J. Math. Pur Appl. 2, 418–436.

Liu, J.-Y., Chen, C.-H., Lin, C.-H., Tsai, H.-F., Chen, C.-H., Kamogawa, M., 2011. Ionospheric disturbances triggered by the 11 march 2011 m9.0 tohoku earthquake. J. Geophys. Res. 116 (A6), A06319.

Magnus, J. R., Neudecker, H., 1988. Matrix differential calculus with applications in statistics and econometrics. Wiley, New York, differential of a determinant, page 149.

Mai, C. L., Kiang, J. F., 2009. Modeling of ionospheric perturbation by 2004 sumatra tsunami. Radio Science 44 (3), RS3011.

Makela, J. J., Lognonné, P., Hébert, H., Gehrels, T., Rolland, L., Allgeyer, S., Kherani, A., Occhipinti, G., Astafyeva, E., Co´isson, P., Loevenbruck, A., Clévédé, E., Kelley, M. C., Lamouroux, J., 2011. Imaging and modeling the ionospheric airglow response over hawaii to the tsunami generated by the tohoku earthquake of 11 march 2011. Geophys. Res. Lett. 38 (24), L00G02.

Masci, F., Thomas, J. N., 2015. On the reliability of the spatial scintillation index to detect earthquake precursors in the ionosphere. Radio Science 50 (8), 745–753.
URL http://dx.doi.org/10.1002/2015RS005734

Mikumo, T., 1968. Atmospheric pressure waves and tectonic deformation associated with the alaskan earthquake of march 28, 1964. J. Geophys. Res. 73 (6), 20092025.

Misner, C. W., Thorne, K. S., Wheeler, J. A., 1973. Gravitation. W. H. Freeman and Company, San Francisco.

Monin, A. S., Yaglom, A. M., 1987. Statistical Fluid Mechanics: Mechanics of Turbulence. Vol. 1. The MIT Press, Cambridge, Mass., section 6.3, p. 389.

Olbers, D. J., 1981. The propagation of internal waves in a geostrophic current. J. Phys. Oceanogr. 11, 1224–1233.

Ostrovsky, L. A., 2008. Ionospheric effects of ground motion: The roles of magnetic field and nonlinearity. J. Atmos. Sol. Terr. Phys. 70, 1273–1280.

Ostrovsky, L. A., Rubakha, N. R., 1972. Nonlinear magnetic sound in a gravitational field. Soviet Radiophysics 15, 986–991.

Peltier, W. R., Hines, C. O., 1976. On the possible detection of tsunamis by a monitoring of the ionosphere. J. Geophys. Res. 81 (12), 1995–2000.

Pokhotelov, O. A., Parrot, M., Fedorov, E. N., Pilipenko, V. A., Surkov, V. V., Gladychev, V. A., 1995. Response of the ionosphere to natural and man-made acoustic sources. Annales Geophysicae 13 (11), 1197–1210.
URL http://www.ann-geophys.net/13/1197/1995/

Pulinets, S., September 2004. Ionospheric precursors of earthquakes; recent advances in theory and practical applications. TAO 15 (3), 413–435.

Rapoport, V., Bespalov, P., Mityakov, N., Parrot, M., Ryzhov, N., 2004. Feasibility study of ionospheric perturbations triggered by monochromatic infrasonic waves emitted with a ground-based experiment. Journal of Atmospheric and Solar-Terrestrial Physics 66 (12), 1011 – 1017.
URL http://dx.doi.org/10.1016/j.jastp.2004.03.010

Rayleigh (John William Strutt), L., 1912. On the propagation of waves through a stratified medium, with special reference to the question of reflection. Proc. Royal Soc. A 86, 207–226.

Varotsos, P., Alexopoulos, K., Lazaridou, M., 1993. Latest aspects of earthquake prediction in Greece based on seismic electric signals, II. Tectonophysics 224 (13), 1 – 37.
URL http://dx.doi.org/10.1016/0040-1951(93)90055-O

Varotsos, P. A., Sarlis, N. V., Skordas, E. S., Oct 2003. Electric fields that "arrive" before the time derivative of the magnetic field prior to major earthquakes. Phys. Rev. Lett. 91, 148501.

Weinberg, S., 1962. Eikonal method in magnetohydrodynamics. Phys Rev. 126, 1899–1909.

Weinberg, S., 1972. Gravitation and Cosmology. John Wiley & Sons, New York.

Wentzel, G., 1926. Eine Verallgemeinerung der Quantenbedingungen für die Zwecke der Wellenmechanik. Z. Phys. 38, 518–529.

Yeh, K. C., Liu, C. H., 1972. Theory of ionospheric waves. Vol. 17 of International Geophysics Series. Academic Press, New York.

Young, J. M., Greene, G. E., 1982. Anomalous infrasound generated by the alaskan earthquake of 28 march, 1964. J. Acoust. Soc. Am. 71 (2), 334–339.

Figure Captions

Figure 1. Dispersion relation for a magneto-acoustic-gravity wave for propagation in the same vertical plane as the Earth's magnetic field. The surface gives the intrinsic frequency in rad s^{-1} as a function of k_x and k_z in km^{-1}. Also shown is the intersection of the surface with a horizontal plane for an intrinsic frequency of 0.001 Hz, which is below the acoustic cutoff frequency for this case. The sound speed, $c_s = 0.3$ km s^{-1}. The acoustic cut-off frequency $\omega_a = 0.0105$ radians s^{-1}. The Brunt-Väisälä frequency, $N = 0.01$ s^{-1}. The angle between the magnetic field and vertical, $\phi = 45°$. The Alfvén speed, $c_A = 0.01$ km s^{-1}. The effect of the magnetic field is smaller here than it is in figure 2 because of the smaller Alfvén speed here. Generally, the effect of the magnetic field increases with height in the atmosphere as the Alfvén speed increases because it is inversely proportional the the square root of density. The value of c_A in this figure corresponds to a height of about 95 km if we use a value of 8.5 km as the density scale height (Ostrovsky, 2008). Color online.

Figure 2. Dispersion relation for a magneto-acoustic-gravity wave for propagation in the same vertical plane as the Earth's magnetic field. The surface gives the intrinsic frequency in rad s^{-1} as a function of k_x and k_z in km^{-1}. Also shown is the intersection of the surface with a horizontal plane for an intrinsic frequency of 0.001 Hz, which is below the acoustic cutoff frequency for this case. The Alfvén speed, $c_A = 0.03$ km s^{-1}. Otherwise, conditions as in figure 1. The effect of the magnetic field is larger here than it is in figure 1 because of the larger Alfvén speed here. Generally, the effect of the magnetic field increases with height in the atmosphere as the Alfvén speed increases because it is inversely proportional the the square root of density. The part of the dispersion relation near the origin corresponds to a gravity wave. The part away from the origin corresponds to a magnetoacoustic wave. Where they join gives the possibility of coupling between the two kinds of waves. The value of c_A in this figure corresponds to a height of about 115 km if we use a value of 8.5 km as the density scale height (Ostrovsky, 2008). Color online.

Figure 3. Dispersion relation for a slow magneto-acoustic-gravity wave for propagation in the same vertical plane as the Earth's magnetic field. The surface gives the intrinsic frequency in rad s^{-1} as a function of k_x and k_z in km^{-1}. This is a slow magnetoacoustic wave. Also shown is the intersection of the surface with a horizontal plane for an intrinsic frequency of 0.01 Hz, which is above the acoustic cutoff frequency for this case. The Alfvén speed, $c_A = 0.25$ km s^{-1}. Otherwise, conditions as in figure 1. The conditions in this figure represent the case where the Alfvén speed c_A is slightly smaller than the sound speed c_s, which would occur at a height of about 152 km in the atmosphere if we use a value of 8.5 km as the density scale height (Ostrovsky, 2008). Color online.

Figure 4. Dispersion relation for a fast magneto-acoustic-gravity wave for propagation in the same vertical plane as the Earth's magnetic field. The surface gives the intrinsic frequency in rad s^{-1} as a function of k_x and k_z in km^{-1}. This is a fast magnetoacoustic wave. Also shown is the intersection of the surface with a horizontal plane for an intrinsic frequency of 0.01 Hz, which is above the acoustic cutoff frequency for this case. The Alfvén speed, $c_A = 0.25$ km s^{-1}. Otherwise, conditions as in figure 1. The conditions in this figure represent the case where the Alfvén speed c_A is slightly smaller than the sound speed c_s, which would occur at a height of about 152 km in the atmosphere if we use a value of 8.5 km as the density scale height (Ostrovsky, 2008). Color online.

Figure 5. Dispersion relation for magneto-acoustic-gravity waves for propagation in the same vertical plane as the Earth's magnetic field for an intrinsic frequency (0.01 Hz) above the acoustic cutoff frequency. The vertical axis is k_z in km s^{-1}. The horizontal axis is k_x in km s^{-1}. The Alfvén speed, $c_A = 0.25$ km s^{-1}. Otherwise, conditions as in figure 1. The center part is a fast magnetoacoustic wave. The outer portion is a slow magnetoacoustic wave. From the lower left to the upper right, the distances from the origin are approximately: ω/c_A, ω/c_s, ω/c_s, and ω/c_A. Because of the effect of gravity, the distances are only approximate. The conditions in this figure represent the case where the Alfvén speed c_A is slightly smaller than the sound speed c_s, which would occur at a height of about 152 km in the atmosphere if we use a value of 8.5 km as the density scale height (Ostrovsky, 2008). If the Alfvén speed c_A and the sound speed c_s were equal, the two branches of the dispersion relation would touch, and there would be coupling between the acoustic waves and the magnetic sound waves. This would occur at a height of about 155 km in the atmosphere because of the exponential growth of C_A with height (Ostrovsky, 2008).

Figure 6. Dispersion relation for magneto-acoustic-gravity waves for propagation in the same vertical plane as the Earth's magnetic field for an intrinsic frequency (0.01 Hz) above the acoustic cutoff frequency. The vertical axis is k_z in km s^{-1}. The horizontal axis is k_x in km s^{-1}. The Alfvén speed, $c_A = 0.35$ km s^{-1}. Otherwise, conditions as in figure 1. The center part is a fast magnetoacoustic wave. The outer portion is a slow magnetoacoustic wave. From the lower left to the upper right, the distances from the origin are approximately: ω/c_s, ω/c_A, ω/c_A, and ω/c_s. Because of the effect of gravity, the distances are only approximate. The conditions in this figure represent the case where the Alfvén speed c_A is slightly greater than the sound speed c_s, which would occur at a height of about 158 km in the atmosphere if we use a value of 8.5 km as the density scale height (Ostrovsky, 2008). If the Alfvén speed c_A and the sound speed c_s were equal, the two branches of the dispersion relation would touch, and there would be coupling between the acoustic waves and the magnetic sound waves. This would occur at a height of about 155 km in the atmosphere because of the exponential growth of C_A with height (Ostrovsky, 2008).